



This is to certify that the
thesis entitled
Thermodynamic Properties of Solvents
at Infinite Dilution in Lignin

presented by

Sherry Lynn McArthur

has been accepted towards fulfillment
of the requirements for

M.S. degree in CHE

A handwritten signature in cursive script, appearing to read "Eric A. Dandekar", written over a horizontal line.

Major professor

Date July 27, 1987



RETURNING MATERIALS:
Place in book drop to
remove this checkout from
your record. FINES will
be charged if book is
returned after the date
stamped below.

--	--	--

THERMODYNAMIC PROPERTIES OF SOLVENTS
AT INFINITE DILUTION IN LIGNIN

By

Sherry Lynn McArthur

A THESIS

Submitted to
Michigan State University
in partial fulfillment of the requirements
for the degree of

MASTER OF SCIENCE

Department of Chemical Engineering

1987

ABSTRACT

THERMODYNAMIC PROPERTIES OF SOLVENTS AT INFINITE DILUTION IN LIGNIN

By

Sherry L. McArthur

The development of products and applications using the variety of forms of lignin existing today requires knowledge of the engineering properties of lignin. The ability to characterize the physical properties of lignin; a complex, noncrystalline, network polymer; is difficult, at best. The solubility properties of lignin are the focus of this study. The method of inverse gas-solid chromatography was employed to investigate the solvent-polymer interactions for 17 different solutes and kraft lignin. Data was collected at 130°C and 160°C for two different column loadings. The retention time data was used to calculate the Flory-Huggins interaction parameter, χ , and the specific interaction parameter, Λ . In conjunction with the solubility parameter at 25°C, the thermodynamic information supported the findings of bench scale solubility tests performed at room temperature. Specifically, the ability of dimethylformamide to solubilize greater than 10% by weight kraft lignin was predicted by the method of inverse gas-solid chromatography.

ACKNOWLEDGMENTS

With appreciation to Dr. Eric A. Grulke for his dedication and patience throughout the duration of this work. For my husband, John, whom without his support the completion of this work would not be possible.

TABLE OF CONTENTS

List of Tables	vi
List of Figures	viii
List of Symbols	ix
I. Introduction	1
1.1. Lignin Morphology, Function, and Occurrence	2
1.2. Delignification via Chemical Pulping	5
1.3. Lignin Applications and Research Motivation	6
II. Literature Review	8
2.1. Current Applications of Lignin	8
2.1.1. Lignin as a Rubber Reinforcer	8
2.1.2. Specialty Chemicals and Chemical Feedstocks	11
2.1.3. Fillers and Extenders	12
2.1.4. Adhesives	14
2.2. Characteristics of Lignin Resulting from HF Saccharification of Wood	18
2.3. Inverse Gas Chromatography	19
2.3.1. Relationships Between the Specific Retention Volume and Thermodynamic Parameters: Mole Fraction Activity Coefficients	22
2.3.2. Weight Fraction Activity Coefficients	25
2.3.3. Effects of Sample Size and Polymer Loading	30
2.3.4. Effects of Polymer Support	31
2.3.5. Two Parameter Thermodynamic Models for χ	32
2.3.6. Dependence of χ on Polymer Chain Branching	34

2.3.7.	Effects of Polymer Degradation	34
2.3.8.	Relationship Between Specific Retention Volume and Molar Gibbs Energy of Absorption	35
2.3.9.	Intermolecular Forces Occurring in Solutions	39
2.3.10.	Relationship Between Specific Retention Volume and Heat of Solution	41
2.3.11.	Evaluating Thermodynamic Data from Inverse GLC	42
2.3.12.	Inverse Gas-Solid Chromatography	42
2.3.13.	Relationship Between Specific Retention Volume and Molar Gibbs Energy of Adsorption	43
III.	Experimental Protocol	45
3.1.	The Glass Transition Temperature and Thermal Stability of Lignin	46
3.1.1.	Differential Scanning Calorimetry	46
3.1.2.	Isothermal Degradation Studies	47
3.2.	Solubility Studies	47
3.3.	Inverse Gas Chromatography	48
3.3.1.	Experimental Apparatus	49
3.3.2.	Probe Molecules and Stationary Phases	49
3.3.3.	Column Preparation	51
3.3.4.	Experimental Procedure	53
IV.	Discussion of Results	56
4.1.	Determination of T_g and Thermal Stability	56
4.2.	Solubility Studies	59
4.3.	Inverse Gas Chromatography	62
4.3.1.	Specific Retention Volume	62
4.3.2.	Physical Properties of Solvents and Calculation of the Flory-Huggins Interaction Parameter	62
4.3.3.	Specific Interaction Parameter Data Analysis	72

4.3.4.	Dependence of Solubility on Thermodynamic Parameters	83
4.3.5.	Dependence of χ and Λ on Operating Conditions	98
V.	Summary and Conclusions	101
	List of References	103

LIST OF TABLES

Table 1.	Potential Applications for Lignin	9
Table 2.	Results of Isothermal Weight Loss Study	58
Table 3.	Effective Solvents for Kraft "Indulin" Lignin [Schuerch, 1952].	59
Table 4.	Results of Solubility Studies by Glasser and coworkers for Kraft lignin ^a [Glasser et al, 1984].	60
Table 5.	Results of Bench Scale Solubility Studies for Kraft REAX 27 Lignin	61
Table 6.	Specific Retention Volume Calculations for 8.4% Coverage of Kraft Lignin at 130°C ($m_2 = 1.511$ g).	63
Table 7.	Specific Retention Volume Calculations for 8.4% Coverage of Kraft Lignin at 160°C ($m_2 = 1.511$ g).	64
Table 8.	Specific Retention Volume Calculations for 3.96% Coverage of Kraft Lignin at 130°C ($m_2 = 0.697$ g).	65
Table 9.	Specific Retention Volume Calculations for 3.96% Coverage of Kraft Lignin at 160°C ($m_2 = 0.697$ g).	66
Table 10.	General Pure Solvent Properties	68
Table 11.	Solvent Molar Volumes and Vapor Pressures	70
Table 12.	Second Virial Coefficients	71
Table 13.	Data Analysis for 8.4% Coverage at 130°C	73
Table 14.	Data Analysis for 8.4% Coverage at 160°C	74
Table 15.	Data Analysis for 3.96% Coverage at 130°C	75
Table 16.	Data Analysis for 3.96% Coverage at 160°C	76
Table 17.	Summary of Results for 8.4% Coverage at 130°C	89
Table 18.	Summary of Results for 8.4% Coverage at 160°C	90

Table 19. Summary of Results for 3.96% Coverage at 130°C	91
Table 20. Summary of Results for 3.96% Coverage at 160°C	92

LIST OF FIGURES

Figure 1.	Lignin's Precursors and a Simplified Representation of Lignin's Structure Including Typical Bonds [Janshekar and Fiechter, 1983]	3
Figure 2.	Schematic of Gas Chromatographic Apparatus	50
Figure 3.	Differential Scanning Calorimetry Traces	57
Figure 4.	ΔG_{ads} vs. α_1 (8.4% coverage, 130°C)	79
Figure 5.	ΔG_{ads} vs. α_1 (8.4% coverage, 160°C)	80
Figure 6.	ΔG_{ads} vs. α_1 (3.96% coverage, 130°C)	81
Figure 7.	ΔG_{ads} vs. α_1 (3.96% coverage, 160°C)	82
Figure 8.	ΔG_{ad} vs. μ_1 (8.4% coverage, 130°C)	84
Figure 9.	ΔG_{ad} vs. μ_1 (8.4% coverage, 160°C)	85
Figure 10.	ΔG_{ad} vs. μ_1 (3.96% coverage, 130°C)	86
Figure 11.	ΔG_{ad} vs. μ_1 (3.96% coverage, 160°C)	87
Figure 12.	A versus χ for 8.4% Coverage and 130°C	94
Figure 13.	A versus χ for 8.4% Coverage and 160°C	95
Figure 14.	A versus χ for 3.96% Coverage and 130°C	96
Figure 15.	A versus χ for 3.96% Coverage and 160°C	97

LIST OF SYMBOLS

a	= experimentally determined coefficient
A_{280}	= absorptivity coefficient of solvent at 280 nm
a_i	= activity of component i
a_1^g	= activity of solvent in gas phase
a_1^s	= activity of solvent in polymer phase
b	= experimentally determined coefficient
B_{11}	= second virial coefficient of component 1 in the gas state
c	= experimentally determined coefficient
f_p	= correction factor for finite pressure drop through column
f_i	= fugacity of component i
f_i^0	= fugacity of component i in the standard state
f_1^g	= fugacity of solvent at initial temperature and pressure in gas phase
f_1^s	= fugacity of solvent in the polymer phase
f_1^{0g}	= fugacity of solvent in standard state of gas
f_1^{0s}	= fugacity of solvent in standard state of polymer
$H_{1,2}$	= Henry's law constant
k_0	= partition coefficient in column
m_2	= weight of lignin contained in column
M_i	= molecular weight of component i

$(\bar{M}_2)_n$	= number average molecular weight of polymer
MW	= molecular weight of solvent
$N_{i, gas}$	= number of moles of solute i in gas phase
$N_{i, liq}$	= number of moles of solute i in liquid phase
P	= total pressure
P_1	= partial pressure of component 1
P_c	= critical pressure of solvent
P_i	= pressure at the inlet to the column
P_i^S	= saturation vapor pressure of component 1
P_o	= pressure at the outlet of the column
Q	= gas flow rate at column outlet corrected to standard temperature
r	= measurement of polymer polydispersity
R	= ideal gas constant
s	= standard deviation
t_g	= retention time of solute
t_r	= retention time of an air sample through column
T	= absolute temperature
T_0	= standard absolute temperature (273.2 K)
T_b	= boiling point of solvent
T_c	= critical temperature of solvent
T_g	= glass transition temperature of polymer on an absolute scale
v_i	= specific volume of component i
$V_{1, gas}$	= volume of component 1 in the gas phase
$(\bar{V}_2)_n$	= number average of molar volumes in a polydisperse polymer
v_g^0	= specific retention volume

V_{gas}	= volume of gas phase in column
V_i	= liquid molar volume of component i
V_{liq}	= volume of liquid phase in column
V_N	= net retention volume corrected for gas hold-up
V_N^0	= net retention time corrected for gas hold-up at zero column pressure
V_R	= retention volume
w_i	= weight fraction of component i
w_2	= weight of polymer loading in column
x_i	= mole fraction of component i
y_1	= mole fraction of solute in gas phase
α_1	= polarizability of solvent
γ_i	= activity coefficient of component i referenced by mole fraction
γ_1^∞	= activity coefficient as $x_1 \rightarrow 0$
δ_1	= solubility parameter
ΔG_{abs}	= molar Gibbs energy of absorption
$-\Delta G_{ad}$	= difference between $-\Delta G_{ads}$ calculated using polarizabilities and that obtained from experiments
ΔG_{ads}	= molar Gibbs energy of adsorption
$-\Delta G_{ads}^*$	= molar Gibbs energy of adsorption calculated from model
ΔG_s	= molar Gibbs energy of sorption
ΔH_s	= heat of solution
$\Delta\mu$	= shift in wavelength due to hydrogen bonding capacity of solvent
Λ	= specific interaction parameter
μ	= dipole moment (Debye)
μ_1	= dipole moment (C-m)

μ_1^g	= chemical potential of solvent at initial temperature and pressure
μ_1^{0g}	= chemical potential of solvent in standard state of the gas phase
μ_1^{0s}	= chemical potential of solvent in standard state of the polymer phase
μ_r	= reduced dipole moment
ϕ_i	= volume fraction of component i
χ	= Flory-Huggins interaction parameter
χ_H	= enthalpy contribution to the Flory-Huggins interaction parameter
χ_s	= entropy contribution to the Flory-Huggins interaction parameter
ω	= acentric factor of solvent
Ω_i	= activity coefficient of component i referenced by weight fraction
Ω_1^∞	= activity coefficient as $w_1 \rightarrow 0$

I. Introduction

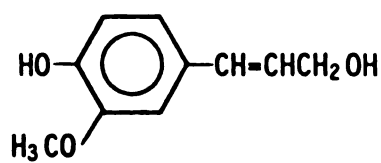
Wood can be described as a composite material made up of three main constituents: cellulose (approximately 42%), lignin (15-36%), and hemicellulose. Although much attention has previously been paid to the utilization of the cellulosic components of wood, until recently few efforts have been directed towards processes which utilize lignin. The reasons why lignin utilization was slow to develop are two-fold. First, lignin is a biopolymer which is quite complex, both physically and chemically. This renders development of structure-property relationships for this macromolecule difficult, at best. Secondly, in the past the low cost of petroleum-based products made several technically feasible lignin-derived products economically unattractive. More recently, however, several factors have arisen that make extensive research directed toward converting lignin to useful end products necessary. The rapid increase in price and uncertainty of supply of petroleum and natural gas makes lignin utilization economically important. Also, recent developments leading to detailed structural schemes and information regarding chemical, physical, and mechanical properties of lignin makes research in this area more promising.

1.1. Lignin Morphology, Function, and Occurrence

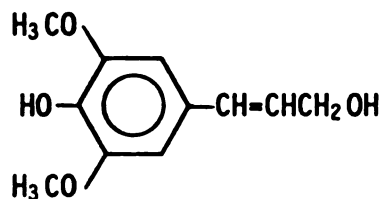
Lignin can be chemically described as a three-dimensional, highly branched polymer made up of phenylpropane units joined together by carbon-carbon bonds and ether linkages [Sarkanen, 1971]. The lignin molecule possesses a variety of functional groups which offer many potential sites for chemical modification and reaction [Sarkanen, 1971]. Native lignin is present as a cell wall constituent in almost all dry-land plants making lignin the most abundant aromatic organic polymer on earth. It is second only in abundance to cellulose [Falkehag et al, 1976]. Within the plant, lignin is a high molecular weight polymer which acts as a "natural adhesive" by binding cells of woody plants together [Sarkanen, 1971]. Lignin imparts rigidity to cell walls and acts as a permanent bonding agent between cells, generating a composite structure outstandingly resistant towards impact, compression, and bending. Lignin also plays a vital role in a tree's vascular system by decreasing the permeation of water across the cell wall; this facilitates transportation of liquids throughout the plant. Additionally, it has been noted that lignin aids in resistance to attack by microorganisms [Sarkanen, 1971].

Native lignin is formed in plants via an enzyme-initiated dehydrogenative polymerization of three primary precursors; trans-coniferyl alcohol, trans-sinapyl alcohol, and trans-p-coumaryl alcohol [Sarkanen, 1971]. The structures of these precursors along with a simplified representation of lignin's chemical structure are shown in Figure 1 [Janshekar and Fiechter, 1983]. Since lignin has no regular repeating monomeric unit,

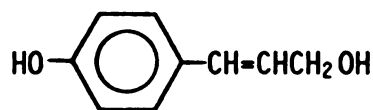
3



trans-coniferyl alcohol

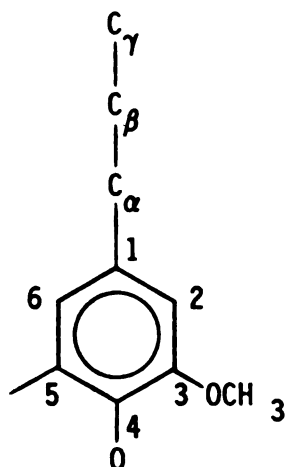


trans-sinapyl alcohol



trans-p-coumaryl

Simplified Lignin Structure



Typical Bonds in Lignin

- β -aryl ether (β -O-4)
- α -aryl ether (α -O-4)
- diphenyl ether (4-O-5)
- α -alkyl ether (α -O- γ)
- biphenyl (5-5')
- β - β
- β -1
- β -5

Figure 1. Lignin's Precursors and a Simplified Representation of Lignin's Structure Including Typical Bonds [Janshekar and Fiechter, 1983]

it is impossible to draw its complete chemical structure. It is sufficient to say that lignin exists as a noncrystalline, network polymer with a phenylpropane backbone linked in a statistically random fashion via a combination of carbon-carbon and ether-type bonds [Drew et al, 1978]. Figure 1 includes a listing of the typical bonds, and the respective codes, which exist to give lignin its complicated structure.

Approximately 40-50 million tons of lignin are produced annually as a by-product of the chemical processing of wood [Falkehag et al, 1976]. Most of this lignin results from chemical pulping processes. The lignin derived from these pulping processes is appropriately designated "technical lignin" and is among the most abundant renewable resources on earth. These large quantities of lignin are usually disposed of as waste materials or concentrated and burned for its fuel value to provide energy for the chemical recovery processes of pulping plants. The fuel value of lignin is 12,700 BTU/lb and represents 40% of the total fuel value of softwood, while lignin only comprises 28% of softwood's dry mass [Drew et al, 1978]. Economically speaking, lignin's fuel value is approximately 3 to 4 cents/lb [Fall, 1979, (Glasser, 1981)]. Since the fuel value of lignin determines its market value, alternative uses of lignin must consider the economics of alternative fuel supply when evaluating feasibility. If alternative uses for lignin derived from pulping processes are found, pulp manufacturers will be forced to utilize other resources for the energy intensive recovery processes in their operations. This means that two factors will control the distribution of lignin resources: 1) the current economic conditions which control the price (ie. the supply and demand) of energy and chemicals, and 2) the

state of technology in the development of processes for efficient utilization of technical lignins.

1.2. Delignification via Chemical Pulping

As previously mentioned, most by-product lignins result from chemical pulp manufacturing. Chemical pulping is a polymer separation process in which defibration of the wood is achieved by dissolving the lignin which binds the cellulosic fibers together [Farmer, 1965]. The result of chemical pulping is delignification of the wood to yield "wood fibers" and an isolated soluble lignin. This isolation method often results in lignin losing most of its adhesive properties. Currently, two chemical pulping processes predominate; the sulfate or Kraft process, and the sulfite process.

The Kraft process is an alkaline process which is employed for 95% of all chemical pulping [Falkehag et al, 1976]. This process can be easily applied to all species of wood. Aryl-ether bonds of lignin are cleaved to delignify the wood producing polyphenolic lignin which is soluble in the highly alkaline kraft pulping liquor. The resultant lignin is called kraft lignin and is highly insoluble under acidic or neutral conditions [Farmer, 1965]. The sulfite process, on the other hand, is an acidic process. Lignin is sulfonated at the alpha carbon atom then depolymerized by the acidic liquor to yield a water-soluble liginosulfonate [Farmer, 1965].

1.3. Lignin Applications and Research Motivation

In 1984 alone, approximately 20 million tons of kraft lignin were produced in the United States [Glasser et al, 1984]. At the present time only relatively small amounts of the technical lignins produced each year are used commercially. Typical applications include use as dispersing and grinding aids, wood adhesives, sequestering agents, water-soluble binders, media for yeast cultures, for vanillin production and for degradation into sulfur-containing compounds [Dolenko and Clarke, 1978].

There are three major categories of research on lignin utilization: 1) direct use of polymeric lignin, 2) utilization of chemically modified lignin, and 3) degradation of lignin to chemical feedstocks or fuels. Lignin applications which would require research in the above areas are: adhesives in wood systems; reinforcers in rubber composites; fillers, extenders, and binders in polymer composites; chemical feedstocks and specialty chemicals. In order to determine the feasibility of using lignin for any of these applications, one must first analyze the engineering properties of lignin.

The engineering properties which must be investigated include: molecular weight distribution, solubility properties, mechanical strength, and thermal stability. Once these properties of a given type of lignin have been established, research can be directed toward applications which require that specific combination of engineering properties.

The emphasis of the work presented here is to establish a technique to determine solubility properties of lignins. The types of lignin included in the investigation are commercially available kraft lignin and HF lignin resulting from hydrogen fluoride saccharification of wood. A technique referred to as "inverse gas chromatography" is employed to qualitatively determine the relative solubility of several solvents in kraft lignin.

II. Literature Review

2.1. Current Applications of Lignin

Since lignin is a low cost, abundant, renewable resource many researchers have attempted to find methods of converting lignin into useful end products. Table 1 summarizes many of the potential uses for a variety of isolated lignins. Each application will be discussed in detail below.

2.1.1. Lignin as a Rubber Reinforcer

Using lignin as a reinforcer in commercial rubbers is not a recent idea. In 1948, the Howard Smith Paper Mills initiated a research program to evaluate the prospect of using lignin as a substitute for carbon black [Raff et al, 1948]. Research prior to this time showed that some reinforcement properties were detected when kraft lignin was incorporated in GR-S rubber [Mischustin, 1940]. Although the strength of this lignin reinforced rubber was not as high as that obtainable with EPC black, the possibility of using lignin for this purpose had several advantages. First, the specific gravity of lignin is approximately 72% of that of EPC black, therefore, a given weight of kraft lignin would provide 1.4 times the volume loading in the rubber as the same weight of carbon black. Secondly, the light tan color of kraft lignin can be easily masked by pigments to provide a wide variety of colors which are not possible with

Table 1. Potential Applications for Lignin

- 1. Direct Use of Isolated Lignin**
 - a. Rubber reinforcer**
 - b. Adhesives and Binders**
 - c. Fillers**
 - d. Extenders**
- 2. Use of a Modified Lignin Molecule**
 - a. Rubber reinforcer**
 - b. Adhesives and Binders**
 - c. Fillers**
 - d. Extenders**
 - e. Chemical feedstocks**
- 3. Use of Lignin Degradation Products**
 - a. Chemical feedstocks**
 - b. Specialty chemicals**
 - c. Extenders**

EPC black. Since masterbatches prepared by dissolving lignin in sodium hydroxide produces a rubber with inferior properties and only moderate reinforcement, the researchers at Smith Mills undertook the development of a suitably modified lignin. The laboratory preparation of masterbatches was done by the Research and Development Division of Polymer Corporation, Limited, Sarnia. The result of this research was an alkaline lignin modified by oxidation reactions. Simple oxidation reactions were continued until the melting point of the modified lignin was at least 240°C. These oxidized lignins were co-precipitated with GR-S latex, compounded, cured and vulcanized. The rubbers obtained from this co-precipitation were found to be comparable to EPC black-reinforced rubbers. One minor drawback was the slower curing times observed for the lignin compounds [Raff et al, 1948].

Braddon and Falkehag [1973] saw similar results for modified lignin if a good dispersion of particulates in the rubber matrix was obtained. Direct dry-blending of "laundered lignin" was successfully demonstrated by two colloid chemists--Ira Puddington and A. F. Sirianni--of Canada's National Research Council [Del Gatto, 1972]. The "laundering" procedure involved a purification step followed by acidification of the lignin at elevated temperatures to "reform" the lignin polymer. The resulting lignin proved to be a highly amorphous polymer which was easily incorporated into styrene-butadiene rubber (SBR) by dry-milling. The "laundered" lignin was also shown to be compatible with other rubbers.

2.1.2. Specialty Chemicals and Chemical Feedstocks

Technical lignins can be converted to low molecular weight specialty chemicals such as vanillin, dimethylsulfoxide (DMSO), phenol and substituted phenols, and benzene and substituted benzenes [Glasser, 1981]. Currently, vanillin and DMSO are manufactured on an industrial scale from lignosulfonates and kraft lignin [Glasser, 1981]. Both of these products are low-volume, high value chemicals and it is economically feasible to produce these even though yields from these processes are quite low. A dramatic increase in demand would encourage researchers to develop more economical processes, but it is expected that this outlet for lignin will remain a low-volume usage.

Pyrolysis, alkali fusion, and hydrogenolysis of lignin will yield phenol and various substituted phenols in low yields [Glasser, 1981]. Although phenol is a high-value raw material at 32 cents/lb [Huibers, 1980], technical limitations are a major roadblock. These limitations include low yields, generally less than 35%, [Schweers, 1969], and the complex reaction mixture that results [Connors et al, 1980; Elder and Soltes, 1979; and Goheen, 1966].

Lignins may also serve as raw materials or chemical feedstocks for synthetic polymers. Research evidence indicates that low molecular weight fractions of lignin and/or its low molecular weight degradation products can be synthesized into thermostable thermoplastics [Lindberg et al, 1975]. Examples of these thermostable polymers include: polyimides [Penttinen, 1970]; polyphenylene oxides [Goheen and Martin, U. S. Patent

3375283 and Forsman, 1972]; and aromatic polyesters [Era and Hannula, 1974]. The polyimides synthesized by Penttinen were from nitrophenols obtained by nitration of lignin. The resulting polymers were thermally stable up to 720 K and exhibited good mechanical strength properties. Formation of polyphenylene oxides was achieved by Goheen and Forsman using the 2,6-disubstituted phenols found in pulping liquors. These substituted phenols represent approximately 0.2% to 1.0% of the liquor and are products of the degradation of lignin. The properties of these polymers were found to be comparable to those commercially produced. Hannula demonstrated that synthesis of aromatic polyesters was possible from vanillin derivatives. Many vanillin derivatives are also found in the pulping liquor as a result of lignin degradation.

Many researchers have demonstrated that lignin and its degradation products can be used as chemical feedstocks for either production of specialty chemicals or synthetic polymers. In the case of chemical feedstocks for synthetic polymer production, only the low molecular weight fraction of the spent liquor is used. Since this fraction is relatively small, these applications would use very little of the abundance of lignin currently available.

2.1.3. Fillers and Extenders

Due to lignin's complexity and the limited knowledge of its chemical structure it has often been classified as a "waste" product of the chemical pulping industry. Using these lignins as cheap fillers has been an outlet for a small fraction of this "waste" for several years. This

application of technical lignins represents a low-value, moderate-volume use. A filler is a material which is incorporated into a system to minimize the cost of the final product. When present in these systems, the filler must have certain properties in common with the principle material. Some characteristics of good fillers are: low reactivity; compatibility with other materials present; good dispersion properties; and similar thermal stability and strength to that of the main constituent. Glass fibers or particles are excellent examples of fillers. Although lignin might find its place among commercial fillers, it will only be competing with consistently low-value materials and therefore, as energy prices rise this application may not be economically feasible.

An extender or modifier is quite similar to a filler but the incorporation of an extender in a system usually requires more technology than that required for filler applications. Using lignin as a reinforcer in rubbers is an extender application that has vast potential as a moderate-value, high volume use. As indicated earlier, research in this area is ongoing.

Using lignins as coreactants in polyurethane systems appears to be an excellent extender application. Hsu and Glasser [1975] have investigated the possibility of coreacting a modified kraft lignin with propylene oxide to yield a lignin polyester-polyether polyol. The polyol is then used in a formulation for a polyurethane foam. The foam resulting from this series of reactions is light in color, high in strength, low in water sorption, and very low in density. All of these properties

indicate that the polyurethane generated by this method is comparable to the foams currently available commercially. The method can be summarized as follows: lignin is copolymerized with maleic anhydride to yield a lignin-maleic anhydride copolymer; the copolymer is then saponified using sodium hydroxide to yield a carboxylated copolymer; oxyalkylation of the carboxylated copolymer results in the polyol described above. Parallel studies were done eliminating the saponification step, but the result was an inferior polyurethane foam. The modification reactions (ie. copolymerization with maleic anhydride and saponification) seem to serve to "soften" the lignin's structural rigidity by grafting maleic anhydride to the lignin. Making the lignin polymer flexible was found to be very important in formulating a successful foam. The researchers indicate that the extent to which the lignin molecule will need to be "softened" will also determine the percentage of lignin that can be utilized in the manufacturing of a commercial polymeric material.

Clarke [1976] evaluated the economics of using the lignin-based polyol for polyurethane foam production. Competitive fossil fuel-derived equivalents to the lignin polyol were selling for 40 to 60 cents/lb, whereas, kraft lignin-based polyester-polyether polyols were estimated to cost 35 cents/lb.

2.1.4. Adhesives

Based on the function of lignin within the tree it is no surprise that lignins isolated from pulping processes have found their greatest applications and, for that reason, their most extensive research, in the

area of binders or adhesives. Most of these applications are in the wood industry. Chow [1983] suggests that since the energy crisis the focus of the wood industry has been on what he refers to as "adhesive self-sufficiency". He indicates that bark, pulp waste liquor and foliage are viable resources which can be used to produce much of the adhesives that the wood industry requires.

Currently, phenol-formaldehyde and urea-formaldehyde adhesives are used by the wood industry for plywood, particleboard, and waferboard (fiberboard) manufacturing. The major advantages of the urea-formaldehyde resins (UF) are their low cost, lack of color, and relatively short curing times [Forss and Fuhrmann, 1979]. Their chief drawbacks are: the formation of a glueline that is not waterproof which limits outdoor applications, and the more recent problem of formaldehyde emissions from particleboard for extended periods of time after production [Kilpelainen et al, 1976].

Phenol-formaldehyde resins (PF), on the other hand, are quite weather resistant, but they are derived from phenol which is an expensive raw material [Forss and Fuhrmann, 1979]. Hsu and Glasser [1976] have prepared an adhesive using a polyurethane resin developed from commercial kraft lignin. The resin was formulated using the same lignin polyester-polyether polyol previously developed for polyurethane foam applications. They tested several adhesive formulations and their results indicate that through the modification reactions the lignin is "reactivated" and it returns to its role as a structural adhesive in woody plants. Several researchers have had success in using kraft lignin and lignosulfonates in

PF resins, therefore, a brief discussion of the current technology will be discussed here.

Shen and Fung [1979] at the Eastern Forest Products Laboratory, Ontario, Canada have developed a process for using spent sulfite liquor (SSL) as a thermosetting binder for exterior grade waferboard. The process involves the use of calcium-based SSL which is acidified with sulfuric acid and then spray-dried to a powder. At only 10% binder content the aspen particleboard obtained was suitable for exterior applications. The market price for this binder was estimated to be 12 cents/lb as compared to 35 cents/lb for liquid PF resin. This indicates that substantial economic gains can be made using this process with only slight additions to production costs due to elevated curing temperatures.

Dolenko and Clarke [1978] have also devised a process to utilize kraft lignin as an adhesive. Their process also calls for modification of the lignin molecule, and incorporation of the lignin with a PF resin. The kraft lignin is first methylolated then precipitated as a fine particle grade methylolated lignin. This lignin is then combined with the PF resin to yield a modified kraft lignin-PF resin. The resin can be formulated as either a dispersion, powder, or solution. The difference between the three forms is simply purity, the dispersion is the least pure and the powder is the most pure. For plywood adhesion the unpurified dispersion or the semi-purified solution was used. The powdered resin was used to prepare waferboard samples. The resulting plywood and waferboard samples were subjected to standard tests and it was found that the resin met the specifications set for PF resins for

plywood but, in the case of waferboard samples, the requirements were exceeded. The estimated cost of this kraft lignin-PF adhesive in which 7 parts lignin are added to 3 parts PF resin is between 17 and 27.5 cents/lb.

Although the above two methods yield promising results, both require chemical modification of the lignin utilized. In the case of Shen and Fung's work the modification is relatively simple, but this is not the case for the work of Dolenko and Clarke. Before the work of Shen and Fung can be commercially feasible it needs to be analyzed for applications in the manufacture of particleboard and waferboard instead of being limited to plywood adhesion.

Two methods of producing adhesives based on lignin "wastes" are currently on the market as commercial products. The first of these is a kraft lignin-based adhesive named KARATEX® developed by The Finnish Pulp and Paper Research Institute [Kilpelainen et al, 1976]. In this adhesive lignin derivatives of high-molecular weight are co-polymerized with PF resin. The development of KARATEX® results in 40 to 70% of the PF resin being replaced by lignin in commercial PF resin adhesives. No lignin modification is required, but an ultrafiltration separation is required to remove all low molecular weight lignin and lignin degradation products. Separation of the liquor by ultrafiltration not only removes the virtually unreactive low molecular weight components, but it also makes it possible to obtain a lignin with constant properties, even when the lignin is isolated from different spent liquors [Forss and Fuhrmann, 1979].

The second commercially available lignin-based adhesive, Tembind®, is being manufactured by Temifibre Incorporated, Canada after being developed at Forintek Laboratories by Dr. Harry Shen and Louis Calve [Go, 1980]. The system is based on spent sulfite liquor and requires no chemical modification. The SSL is collected, concentrated to approximately 50% solids and is ready for use in waferboard formation. It can also be spray dried at this point to yield a fine powder. Ultrafiltration may be employed if a superior waferboard is needed, but this is not necessary to obtain waferboards comparable to those already produced using PF resins. The Tembind® system is expected to save \$22 to \$26 per ton of waferboard. At a daily production rate of 250 tons per day, the total savings per year will be over \$2 million. This process is very efficient and results in an economically feasible use for lignin as a byproduct of pulp manufacturing.

2.2. Characteristics of Lignin Resulting from HF Saccharification of Wood

The biomass conversion technique currently being studied by Hawley and coworkers at Michigan State University is hydrogen fluoride (HF) saccharification. Currently, the researchers are investigating the gaseous phase reaction, but in the past extensive information has been collected for the liquid HF system [Selke et al, 1982]. Typical experiments employ 1 gram of wood (Bigtooth Aspen, *Populus grandidentata*) and 10 ml of HF at 0°C. After reacting for 1 hour the excess HF is removed by evacuation at elevated temperatures. Water is then added, yielding a water-soluble sugar fraction and an insoluble lignin fraction. The two fractions are separated by centrifugation and analyzed for

fluoride content. To determine the amount of fluoride incorporated into the lignin fraction (HF lignin) the lignin is first degraded via alkali fusion and then analyzed using a fluoride electrode. After one water washing the fluoride level was less than 0.2 mg/gram [Smith et al, 1983]. Levels as low as 0.03 mg fluoride/gram of wood were obtained when the lignin residue was crushed, washed, and dialyzed. The researchers thus concluded that there was "no significant degree of fluorination of the lignin." In addition, preliminary studies indicated that condensation reactions, or changes in lignin's structure, were not occurring and that the lignin was retaining a high degree of functionality.

Further studies on the yields of syringaldehyde and vanillin after alkaline nitrobenzene or alkaline cupric oxide oxidation of HF lignin showed that some condensation of the lignin was occurring due to exposure to HF [Smith et al, 1983]. Defaye and coworkers [1983] studied extensively possible condensation reactions and, in particular, cleavage of aryl-alkyl ether linkages and condensation with carbohydrates (autocondensation). Their studies indicate that neither ester nor ether linkages are cleaved by HF but extensive temperature-dependent and reaction time-dependent autocondensation takes place.

2.3. Inverse Gas Chromatography

The technique of gas-liquid chromatography (GLC) has been well established as a method to accurately determine thermodynamic properties of binary solutions in which the components differ in volatility. Although polymeric materials have typically served as the stationary

phase in GLC, the chromatograms have provided information about the injected sample only. Until recent developments little thermodynamic information was obtained about the non-volatile stationary component of the chromatograph column.

While investigating the solution properties of poly(N-isopropylacrylamide), Olav Smidsrod and J. E. Guillet [1969] used gas chromatography to study solvent-polymer interactions. Using the polymer of interest as the stationary phase they were able to determine the glass-transition temperature, T_g , with an equivalent degree of accuracy as a differential scanning calorimeter. Their work represents the first reported study into the structure of polymers and their interactions with molecules of significantly lower molecular weight using gas chromatography. They succeeded in demonstrating that gas chromatography is a versatile tool useful for determining first- and second-order phase transitions, degrees of crystallinity, and other physical characteristics of a macromolecule. The authors also suggested that the simplest application of gas-liquid chromatography theory would afford the activity coefficients of the solvent at infinite dilution in the polymer.

A review of the initial progress in the field of inverse gas chromatography was included as a chapter in Purnell's Progress in Gas Chromatography [Guillet, 1973]. The chapter reviews the thermodynamics of inverse gas chromatography as well as applications which had already been described in the literature. Beyond infinite dilution activity coefficients and interaction parameters he describes the usefulness of the technique for studying glass transition phenomena, determining

crystallinity in macromolecules, investigating surface properties of polymers, and estimating diffusion constants. He also suggests that GLC could be used to follow the effects that the amount of crosslinking will have on polymer-solvent interactions.

As scientists recognized inverse gas chromatography as a rapid, versatile analytical method for studying polymer-solvent interactions research on specific industrial applications began. Thermodynamic data on commercially available, high-volume, polymers in several solvents was collected and reported by Newman and Prausnitz [1973]. The polymers studied included low density polyethylene, ethylene-vinyl acetate copolymer, ethylene-propylene copolymer, and polyisobutylene. The primary focus of their work was to provide the fundamental thermodynamic data necessary to evaluate devolatilization techniques for polymer solutions and films. This work represents the first of many to supply industry the much sought after polymer-solvent solubility data.

2.3.1. Relationships Between the Specific Retention Volume and Thermodynamic Parameters: Mole Fraction Activity Coefficients

Several researchers using inverse gas chromatography noted a difficulty in applying the theory due to the inherent need to specify the exact molecular weight of the polymeric stationary phase. Patterson and coworkers, including James Guillet, resolved this problem by replacing the reference function of the activity coefficient, mole fraction (x_1), with weight fraction (w_1). A development of the pertinent thermodynamic equations is outlined below [Patterson et al, 1971].

The important pieces of information obtained from a GLC chromatogram are the retention time and retention volume. The retention time, t_g , is defined as the time needed for component 1 to traverse the chromatograph column. The volume of carrier gas which passes through the column in that same time period is referred to as the retention volume, V_R . The net retention volume is defined as,

$$V_N = V_R - V_{gas} \quad (1)$$

where V_{gas} is the volume of gas occupying the column at time zero, often referred to as gas hold-up. For applications involving thermodynamic theory the value of gas hold-up is extrapolated to zero column pressure [Patterson et al, 1971]. This results in the net retention volume expressed as V_N^0 . The partition coefficient, k_0 , is defined by

$$k_0 = \frac{N_{1,liq}}{V_{liq}} \frac{V_{gas}}{N_{1,gas}} \quad (2)$$

and is determined from GLC data by

$$k_0 = \frac{V_N^0}{V_{liq}} \quad (3)$$

The variables $N_{1,liq}$ and $N_{1,gas}$ represent the number of moles of solute in the liquid and gas phases, respectively, and V_{liq} is the volume of the molten polymer phase. Since the quantity k_0 characterizes the partitioning of component 1 between the gas and liquid phases it will decrease rapidly as temperature is increased. Combination of equations 2 and 3 yields,

$$N_{1,\text{gas}} = \frac{N_{1,\text{liq}} \cdot V_{\text{gas}}}{V_N^0} \quad (4)$$

The partition coefficient can be converted to a thermodynamic quantity which represents the interaction between two components in a liquid phase; the activity coefficient is defined as,

$$\gamma_1 = \frac{a_1}{x_1} = \frac{f_1}{(x_1 f_1^0)} \quad (5)$$

where the activity (a_1) is defined as the ratio of the fugacity (f_1) to the fugacity of pure component 1, f_1^0 .

Under ideal gas conditions,

$$f_1 = P_1 ; \quad f_1^0 = P_1^S ; \quad V_{1,\text{gas}} = \frac{RTN_{1,\text{gas}}}{P_1}$$

which leads to

$$\gamma_1 = \frac{P_1}{x_1 P_1^S} = \frac{RTN_{1,\text{gas}}}{V_{1,\text{gas}} x_1 P_1^S} \quad (6)$$

Substitution of equation 4 into equation 6 yields

$$\gamma_1 = \frac{RTN_{1,\text{liq}}}{x_1 P_1^S V_N^0} \quad (7)$$

As the mole fraction, x_1 , approaches zero equation 7 becomes

$$\gamma_1^\infty = \frac{RTN_{2,liq}}{P_1^S V_N^0} \quad (8)$$

Using the virial expansion equation of state to correct for finite pressure, P_1^S , on the chemical potential, equation 8 becomes

$$\ln \gamma_1^\infty = \ln \frac{RTN_{2,liq}}{P_1^S V_N^0} - \frac{P_1^S}{RT} [B_{11} - V_1] \quad (9)$$

Here B_{11} is the gas-state second virial coefficient of component 1 and V_1 is the liquid molar volume.

If the specific retention volume, V_g^0 , which is equal to V_N^0 per gram of liquid phase, is corrected to 0°C the following definition is obtained

$$V_g^0 = \frac{V_N^0}{\text{grams of polymer}} \frac{T_0}{T} \quad (10)$$

Substitution of the definition of the specific retention volume (equation 10) into equation 9 gives

$$\ln \gamma_1^\infty = \ln \frac{(273.2)R}{P_1^S V_g^0 M_2} - \frac{P_1^S}{RT} [B_{11} - V_1] \quad (11)$$

The quantity M_2 is the molecular weight of component 2 and the specific retention volume is calculated from GLC datum using

$$V_g^0 = Q[t_g - t_r] \frac{273.2}{T} \frac{1}{W_2} f_p \quad (12)$$

Since there is a finite pressure drop through the column a correction factor, f_p , is needed where

$$f_p = \frac{[P_i/P_0]^2 - 1}{[P_i/P_0]^3 - 1} \quad (13)$$

The quantity Q is the flow rate at the column outlet; T is the temperature in Kelvin; t_r is the retention time of a pure air sample; W_2 is the weight of polymer loading in the column; P_i is the pressure at the column inlet; and P_0 is the pressure at the column outlet.

2.3.2. Weight Fraction Activity Coefficients

Using equation 11 to determine the activity coefficient of component 1 at infinite dilution in a polymer system is difficult since the equation requires an exact value for M_2 , the molecular weight of the polymer. Defining the molecular weight for a polydisperse macromolecule further complicates obtaining this value.

Patterson and coworkers circumvent this difficulty by first noting that, intuitively, it is unacceptable that $\ln \gamma_1^\infty$ depend increasingly on the polymer molecular weight. This would imply that as $M_2 \rightarrow \infty$, $\ln \gamma_1^\infty \rightarrow -\infty$. They acknowledge the fact that the choice of mole fraction, x_1 , as a reference function is inappropriate and instead choose weight fraction, w_1 .

Development of the relationship between the specific retention volume and the activity coefficient at infinite dilution referenced by weight

fraction, Ω_1^∞ , is analogous to that for γ_1 [Patterson et al, 1971]. By definition,

$$\Omega_1 = \frac{f_1}{f_1^0} \frac{1}{w_1} = \frac{a_1}{w_1} \quad (14)$$

If the gas phase behaves ideally the activity coefficient becomes

$$\Omega_1 = \frac{P_1}{P_1^S} \frac{1}{w_1} = \frac{RTN_{1,gas}}{V_{1,gas} P_1^S w_1} \quad (15)$$

Substitution of equation 4 yields

$$\Omega_1 = \frac{RTN_{1,liq}}{P_1^S w_1 V_N^0} \quad (16)$$

As the weight fraction, w_1 , approaches zero the activity coefficient is expressed as

$$\lim_{w_1 \rightarrow 0} \Omega_1 = \frac{RTN_{2,liq} M_2}{M_1 P_1^S w_1 V_N^0} \quad (17)$$

Substitution of the virial expansion equation of state yields

$$\ln \Omega_1^\infty = \ln \frac{RTN_{2,liq} M_2}{M_1 P_1^S w_1 V_N^0} - \frac{P_1^S}{RT} [B_{11} - V_1] \quad (18)$$

Rearrangement using the definition of the net retention volume in equation 10 gives

$$\ln \Omega_1^\infty = \ln \frac{273.2R}{P_1^S V_g^0 M_1} - \frac{P_1^S}{RT} [B_{11} - V_1] \quad (19)$$

Equation 19 allows for measurement of polymer-solvent interactions without exact information about M_2 or the polydispersity. This is not to say that $\ln (a_1/w_1)^\infty$ does not depend on these factors; the dependence lies in the value of the observed retention volume, V_g^0 .

The development of equation 19 demonstrates that the method of GLC can be used to rapidly evaluate the thermodynamics of polymer solutions. It is, therefore, very desirable to equate the GLC data to the Flory-Huggins interaction parameter, χ .

The activity of a component in a solution can be described statistically as the sum of two contributions: (i) a combinatorial entropy, and (ii) a non-combinatorial free energy of mixing. Combining Flory-Huggins theory with this statistical definition yields

$$\begin{aligned} \ln a_1 &= (\ln a_1)_{\text{comb.}} + (\ln a_1)_{\text{noncomb.}} \\ &= [\ln \phi_1 + (1 - 1/r)\phi_2] + \chi\phi_2^2 \end{aligned} \quad (20)$$

where ϕ_1 and ϕ_2 are volume fractions given by

$$\phi_1 = \frac{w_1 V_1}{w_1 V_1 + w_2 V_2} \quad (21)$$

For polydisperse polymers, r is defined as

$$r = \frac{(\bar{V}_2)_n}{V_1} = \frac{(\bar{M}_2)_n v_2}{V_1} \quad (22)$$

where $(\bar{V}_2)_n$ is the number average of the molar volumes in the polydisperse polymer sample, V_1 is the molar volume of the solvent, $(\bar{M}_2)_n$ is the number average molecular weight of the polymer, and v_2 is the specific volume of the polymer.

For the limiting case where $\phi_2 \rightarrow 1$, equation 20 becomes

$$\ln \Omega_1^\infty = \ln (a_1/w_1)^\infty = \ln \frac{V_1}{v_2} + \left[1 - \frac{V_1}{\bar{M}_2 v_2}\right] + \chi \quad (23)$$

and combination of equations 19 and 23 gives

$$\chi = \ln \frac{273.2 R v_2}{P_1^S v_g^0 V_1} - \left[1 - \frac{V_1}{\bar{M}_2 v_2}\right] - \frac{P_1^S}{RT} [B_{11} - V_1] \quad (24)$$

Equation 24 represents the desired relation between the interaction parameter and experimental GLC information, namely, v_g^0 .

Since the expansion of GLC thermodynamic relationships to polymer-solvent interactions, many researchers have completed experimentation on a variety of systems. Gray and Guillet [1972] used what Guillet describes as the "molecular probe" technique to determine adsorption isotherms for poly(methyl methacrylate) and polystyrene. Guillet [1970] describes his experiments as "sending a pulse of molecules along a narrow tube which has a thin coating of the polymer to be investigated covering

the inner wall". This represents the first time inverse gas chromatography was used to investigate polymer-solvent interactions below the glass transition temperature. The technique in this case is referred to as gas-solid chromatography (GSC).

The chromatography column can be prepared in two ways: (1) coat the inside of the tube with a thin layer of the polymer (capillary) or (2) pack a column with the polymer dispersed as a thin film on an inert support. If the experimenter works at a temperature at or above T_g , the glass transition temperature of the polymer, it is considered gas liquid chromatography. Operation below T_g , where the crystallinity of the polymer molecule remains intact, is referred to as gas-solid chromatography (GSC).

Summers and coworkers [1972] used GLC to study sorption of various hydrocarbons on poly(dimethyl siloxane) (PDMS). In their work they neglected the contribution to χ due to the polydispersity and developed an analogous expression for the interaction parameter using reduction parameters. The resulting equation using asterisks to indicate hard-core volumes for the two components is

$$\chi^* = \ln \frac{273.2 R v_2^*}{P_1^S v_g^0 v_1^*} - 1 - \frac{P_1^S}{RT} [B_{11} - V_1] \quad (25)$$

They used their data to compare experimental χ values from GLC with those obtained from conventional swelling experiments. They concluded that the results using GLC were reliable and in close agreement with those previously determined from static equilibrium absorption experiments.

2.3.3. Effects of Sample Size and Polymer Loading

Newman and Prausnitz [1972] used GLC to determine both the activity coefficients at infinite dilution and the interaction parameters of several solvents in polystyrene. They utilized a packed column with polystyrene coated on various inert supports. Again favorable results were obtained when comparisons were made with static measurements, but the most interesting aspect of their work was the attention paid to various experimental parameters. Firstly, they investigated sample size effects. It was found that the peak maximum retention time was independent over a sample size range of 0.001 to 0.1 μ l. Secondly, it was found that activity coefficients were independent of polymer loading up to coverage ratios of 20%. Even at this relatively high loading changing the carrier gas flow rate by a factor of three did not change specific retention volumes. Thirdly, the possibility of the solid support influencing the data was examined. It was found that polar solvents give rise to asymmetric peaks and a sample size dependence when the support is a diatomaceous earth such as Chromosorb. A solid support such as Fluoropak 80® (powdered polytetrafluoroethylene) produced symmetric peaks with both polar and nonpolar solvents with no evidence of sample size dependence.

Brockmeier and coworkers [1972] extended the theory to enable determination of distribution isotherms, activity coefficients and interaction parameters at finite concentrations. The systems they studied included polystyrene, amorphous polyethylene and atactic polypropylene with selected hydrocarbons. They found that in the limit

of infinite dilution the values of the activity coefficients and the interaction parameters were acceptable. Furthermore, the values of the activity coefficients, Ω_1 , were usually within 5% of the calculated values based on Flory-Huggins and Maron theories. The experimental method they employed has the advantage of providing information on the concentration dependence of the activity coefficient but suffers by being much more complicated and time consuming.

2.3.4. Effects of Polymer Support

Further studies by Newman and Prausnitz [1973] utilized inverse gas chromatography to study the drying of polymer coating films. The objective of their work was to obtain solvent volatility data in polymer coatings when solvent concentration was very low. Their experimental efforts afforded thermodynamic data for 91 binary polymer-solvent systems in the temperature range of 50°C to 200°C. They investigated the occurrence of asymmetric peaks for polar solvents when the support was diatomaceous earth. Evidence that interaction with the solid support was occurring manifested itself as a sample size dependence on retention time. When Fluoropak 80® was used, there was no dependence on sample size and, therefore, symmetric peaks. Conder [1971] states that symmetric peaks do not necessarily guarantee that no adsorption is occurring on the polymer or support. He proposed a model which defines two contributions to the retention volume. One contribution is adsorptive and is proportional to surface area. The other contribution is absorptive and is proportional to the mass of the polymer present. In order that surface effects be eliminated, the coverage ratio (mass of

polymer/mass of support) should be large. As mentioned previously, Newman and Prausnitz [1972] demonstrated that coverage ratios greater than 15% provided accurate, consistent results.

2.3.5. Two Parameter Thermodynamic Models for χ

The data collected by Newman and Prausnitz included several polymers and twenty-one solvents. The studies were run with the polymer above its glass-transition temperature [Newman and Prausnitz, 1973]. They further extended the theory to include molecular contributions by examining more closely the Flory-Huggins interaction parameter. Flory [1953] recognized that the parameter χ includes both an entropic and enthalpic contribution;

$$\chi = \chi_s + \chi_H \quad (26)$$

The entropy contribution, χ_s , arises from the different states of volumetric expansion of the polymer and solvent [Patterson, 1969]. In a binary system the solvent will be much more expanded than the polymer; the free volume of the solvent will be larger than that of the polymer. When two fluids are mixed with significantly different free volumes, the solution is nonideal. For common polymer solutions the nonideality is represented by a χ_s value between 0.3 and 0.4 [Patterson, 1969].

The enthalpic contribution evolves from the intermolecular forces between the solvent and polymer. A negative or low positive value of χ_H indicates that formation of a polymer-solvent solution is favorable. On

the other hand, a relatively high positive value of χ_H predicts that the polymer is insoluble in the solvent.

If equation 23 is substituted with the contributory definition of the interaction parameter and the assumption that $1/r$ will be much less than 1 is invoked,

$$\ln \Omega_1^\infty = \ln \frac{v_1}{v_2} + 1 + \chi_S + \chi_H \quad (27)$$

If χ_S is assumed to be equal to 0.4 equation 27 becomes

$$\ln \Omega_1^\infty = \ln \frac{v_1}{v_2} + 1.4 + \chi_H \quad (28)$$

For the systems used in Newman's and Prausnitz's work the quantity $(v_1/v_2) \approx 1$ and contributes very little to the activity coefficient. Ignoring the enthalpic contribution to χ gives $\ln \Omega_1^\infty = 1.4$; this translates to $\Omega_1^\infty = 4$. Since the majority of the activity coefficients determined in their study had values in the range of 4 to 8, they concluded that the value of the activity coefficient is determined mainly by entropic considerations, ie. differences in free volume. They do, however, acknowledge enthalpic contributions in the form of dispersion forces, permanent dipole-induced dipole interactions, and dipole-dipole interactions [Newman and Prausnitz, 1973].

2.3.6. Dependence of χ on Polymer Chain Branching

Schreiber, Tewari, and Patterson [1973] used inverse gas chromatography to investigate the effects of chain branching in macromolecules on solvent-polymer interactions. This was accomplished by simultaneously studying linear polyethylene (LPE) and branched polyethylene (BPE) with a variety of linear and branched low molecular weight hydrocarbons. An interesting observation during the course of their work was that a complex recrystallization and fractionation sequence takes place when dilute polyethylene solutions are slowly heated. Since much of the data previously reported in the literature on χ values for polyethylene were obtained by visual crystallite disappearance indicating the polymer solution temperature, the authors suggest a reevaluation of the validity of these quantities. Their work provides further evidence that inverse GLC may prove useful for the study of polymer thermal transitions beyond the glass transition temperature.

2.3.7. Effects of Polymer Degradation

Chang and Bonner [1975] determined activity coefficients of benzene in poly(ethylene oxide) (PEO) for a concentration range of 0% to 20% by weight and 70°C to 150°C. Their work represents a thorough compilation of activity data for a commercially important polymer over a wide range of concentration and temperature. The effect of polymer degradation during experimentation was discussed and mathematically evaluated as it pertains to the characteristics of the solution formed and the true polymer loading in the column. Since PEO degrades easily, this effect

can be significant, but for many polymers, little degradation is observed at elevated temperatures. Their results compare favorably with literature values from static tests and a good correlation was found with theoretical values obtained using the corresponding-states theory for polymer solutions developed by Prigogine and coworkers [1957]. Prigogine theory goes beyond the Flory-Huggins theory in that it accounts for non-combinatorial contributions in a more rigorous manner.

2.3.8. Relationship Between Specific Retention Volume and Molar Gibbs Energy of Absorption

The raw data obtained from inverse gas chromatography has been used by many researchers to determine activity coefficients as well as Flory-Huggins interaction parameters. When researchers recognized that this method was a powerful analytical tool for investigation of polymer-solvent interactions, the theory was expanded to allow for calculation of a variety of thermodynamic quantities.

Dincer and Bonner [1978] used the same raw data to calculate other thermodynamic quantities such as heats of solution and Gibbs energies of absorption. The system studied was an ethylene-vinyl acetate copolymer with 43 solvents at both 150.46°C and 160.53°C. It was illustrated how the interactions between the solvent and polymer can be resolved into contributions from dispersion forces, polar forces, and specific interactions. This type of analysis provides an alternative to the semiquantitative Hansen three-dimensional solubility parameter approach. The development of pertinent equations for molar Gibbs energy of

absorption and the heat of solution will be described below [Dangayach et al, 1981].

The change in the chemical potential of a solvent initially at temperature T and pressure P to the standard state in the polymer phase, s , is

$$\mu_1^s - \mu_1^{0s} = RT \ln \frac{f_1}{f_1^{0s}} = RT \ln a_1^s \quad (29)$$

In the same manner the change in chemical potential of a solvent at temperature T and pressure P to the standard state in the gas phase (g) is given by

$$\mu_1^g - \mu_1^{0g} = RT \ln \frac{f_1^g}{f_1^{0g}} = RT \ln a_1^g \quad (30)$$

At equilibrium the chemical potentials of the solvent in the gas phase and the polymer phase are equal, $\mu_1^s = \mu_1^g$, and subtracting equation 29 from equation 30 gives

$$\mu_1^{0s} - \mu_1^{0g} = RT \ln a_1^g - RT \ln a_1^s \quad (31)$$

The definition of the molar Gibbs energy of absorption is $-\Delta G_{\text{abs}} = \mu_1^{0g} - \mu_1^{0s}$, which leads to

$$-\Delta G_{\text{abs}} = RT \ln \frac{a_1^s}{a_1^g} \quad (32)$$

The standard state of the solvent in the gas phase is defined as pure solvent at 1 atmosphere and the temperature of interest. It is assumed that the solvent is sufficiently dilute in the polymer phase, therefore, Henry's law is obeyed. The standard state of the polymer phase is hypothetical for solvents which do not form solutions.

Henry's law constant is defined as

$$H_{1,2} = \lim_{w_1 \rightarrow 0} \frac{f_1^S}{w_1} \quad (33)$$

where f_1^S is the fugacity of the solvent in the polymer phase. When equation 33 is combined with the definition of the activity coefficient referenced to weight fraction we get

$$a_1^S = \frac{f_1^S}{f_1^{0S}} = \frac{f_1^S}{H_{1,2}} = w_1 \quad (34)$$

The gas phase activity can be approximated by partial pressure since the gas will behave ideally at low pressures and high temperatures;

$$a_1 = \frac{f_1^g}{f_1^{0g}} = \frac{p_1}{p_1^S} = \frac{p_1}{1 \text{ atm}} \quad (35)$$

Combining equations 32, 34, and 35 yields

$$-\Delta G_{\text{abs}} = RT \ln \frac{w_1}{p_1/(1 \text{ atm})} \quad (36)$$

From the definition of the net retention volume (equation 3) we have

$$V_N^0 = k_0 V_{liq} = \frac{N_{1,liq}}{V_{liq}} \cdot \frac{V_{gas}}{N_{1,gas}} V_{liq} \quad (37)$$

Combination of equation 37 with the definition of the specific retention volume (equation 10) yields

$$\begin{aligned} v_g^0 &= \frac{T_0}{T} \frac{N_{1,liq}}{N_{1,gas}} \frac{V_{gas}}{\text{gram of polymer phase}} \\ &= \frac{T_0}{T} \frac{\frac{\text{gram solvent in polymer phase}}{\text{gram of polymer phase}}}{\frac{\text{gram solvent in gas}}{\text{ml of gas at } T}} \end{aligned} \quad (38)$$

If there is very little solvent compared to polymer, and the gas behaves ideally, equation 38 can be expressed as

$$v_g^0 = \frac{T_0}{T} \frac{w_1 RT}{y_1 P M_1} = \frac{w_1 R T_0}{P_1 M_1} \quad (39)$$

Substitution of equation 39 into equation 36 leads to an expression for the molar Gibbs energy of absorption in terms of the specific retention volume,

$$-\Delta G_{abs} = RT \ln \frac{M_1 v_g^0}{R T_0 / (1 \text{ atm})} \quad (40)$$

2.3.9. Intermolecular Forces Occurring in Solutions

Models can be proposed for thermodynamic quantities such as the molar Gibbs energy of absorption and the heat of solution by understanding the types of intermolecular forces which can occur between molecules. These forces, also called van-der-Waals-forces, can be classified in two distinct categories. The first category is comprised of directional, induction, and dispersion forces which are non-specific and cannot be completely saturated. In the second group are found hydrogen bonding forces and the forces of charge transfer or electron-pair donor acceptor forces. The latter group of interactions are specific, directional forces which can be saturated and lead to molecular compounds. Each group will be discussed in more detail in the following paragraphs.

Molecules which are electrically neutral but possess an unsymmetrical charge distribution are said to have a permanent dipole moment, μ_1 . Most common organic solvents have permanent dipole moments. Exceptions to this include some hydrocarbons and symmetrical compounds such as carbon tetrachloride and benzene.

Dipole-dipole forces are non-specific directional forces. The magnitude of this force depends on the electrostatic interaction between two molecules which possess permanent dipole moments due to their unsymmetrical distribution of charge. Additionally, temperature has an effect on the magnitude of the dipole-dipole interactions. As temperature increases, the orientations of the molecules becomes statistically random resulting in decreasing potential energy.

Dipole-induced dipole forces arise when the electric dipole of a molecule possessing a permanent dipole moment, μ_1 , induces a dipole moment in a neighboring molecule. An induced moment will always lie in the direction of the inducing dipole and is independent of temperature. The degree to which an induced moment can occur in a given molecule is a function of the polarizability, α_1 , of the apolar molecule.

Instantaneous dipole-induced dipole forces are the result of the continuous electron movement in molecules which do not possess permanent dipole moments. At any instant in time a small dipole moment can polarize the electron system of neighboring molecules. This interaction is also a function of the polarizability of the molecules involved.

Hydrogen bonding is a specific interaction that occurs between molecules which contain hydroxyl groups or groups with a hydrogen atom bound to an electronegative atom. There is no general agreement as to the best way to describe the nature of hydrogen bonds. For the purposes of this work it will suffice to describe it as a dipole-dipole or resonance interaction.

Electron pair donor-electron pair acceptor complexes are the result of charge transfer from the donor to the acceptor molecule. In general these forces are small when compared to non-specific van-der-Waals-forces but can be a contributing factor in solubility.

2.3.10. Relationship Between Specific Retention Volume and Heat of Solution

The heat of solution (ΔH_s) of solvent vapors on the polymer can be determined from V_g^0 using the following relationship [Dwyer and Karim, 1975],

$$\frac{\Delta H_s}{RT^2} = \frac{\partial}{\partial T} [\ln V_g^0] \quad (41)$$

As pointed out by Dwyer and Karim, equation 41 represents an approximate value of ΔH_s . They note that uncertainties in the values of polarizability and dipole movements discourages further refinement of equation 41.

A model for the heat of solution proposed by Dwyer and Karim can be used to identify the various types of intermolecular forces between a polymer and solute in solution. The basis for the model can be expressed as

$$-\Delta H_s = f(\alpha_1, \mu_1) + \Lambda \quad (42)$$

The solute polarizability, α_1 , is a measure of the dipole moment induction a solute will undergo due to an applied electric field. The quantity, μ_1 , is the dipole moment of the solute and should not be confused with the chemical potential. The specific interactions discussed above are contained in the single parameter, Λ . The model of Dwyer and Karim is

$$-\Delta H_s = a\alpha_1 + b\mu_1 + \Lambda \quad (43)$$

where a and b are experimentally determined constants.

2.3.11. Evaluating Thermodynamic Data from Inverse GLC

Interpretation of the thermodynamic data allows one to draw conclusions as to the solubility of a particular solute in a polymer. The analysis is similar to the Hansen's three-dimensional solubility parameter. A negative or near-zero value of the Flory-Huggins interaction parameter indicates favorable interaction between the polymer and solvent.

Additionally, a high positive specific interaction value (Λ) indicates that there do exist interactions between the polymer and solvent. Dincer and Bonner [1978] conclude that no single parameter can be used to determine whether a specific polymer and solute will form a solution. They do, however, point out that values of Λ , χ , and the solute solubility parameter, δ_1 , can be used simultaneously to understand solvent-polymer interactions better.

Karim and Bonner [1978] used equation 41 to estimate the heats of solution of solutes in poly(ethyl methacrylate) at infinite dilution. Using the values for $-\Delta H_s$, Λ , χ , δ_1 , as well as, Ω_1^∞ , they were able to demonstrate that inverse gas chromatography can be used to reliably predict dissolution of a polymer by a solvent.

2.3.12. Inverse Gas-Solid Chromatography

Galín and Rupprecht [1978] completed the first study using both GLC and GSC to investigate the interactions of a commercially important polymer with a variety of solutes above and below the glass transition temperature. In addition, they studied the effects of chain structure by

using both linear and branched polystyrene. Below T_g , non-solvent probes were used so that interactions were restricted to adsorption phenomena only. This allows for estimation of the specific surface area of the inert support accessible to the polymer and therefore, coverage ratio effects can be easily identified.

Dincer and Bonner [1978] used GSC to study the solubility of organic solvents in polyquinoxaline (PQF). From the specific retention volumes, they were able to calculate the molar Gibbs energy of adsorption, χ , and a specific interaction parameter for 40 organic solvents and PQF. The thermodynamic equations describing GSC are derived in much of the same manner as those for gas-liquid chromatography and therefore, they will only be outlined here.

2.3.13. Relationship Between Specific Retention Volume and Molar Gibbs Energy of Adsorption

The molar Gibbs energy of adsorption is related to V_g^0 by

$$\Delta G_{ads} = RT \ln \frac{M_1 V_g^0}{RT_0 / (1 \text{ atm})} \quad (44)$$

In a manner very similar to the development by Dwyer and Karim for the heat of solution, ΔG_{ads} can be expressed empirically as

$$\Delta G_{ads} = a\alpha_1 + b\mu_1 + c + \Lambda \quad (45)$$

where Λ is the specific interaction parameter and a , b , and c are experimentally determined constants. The relationship for the Flory-

Huggins interaction parameter is no different than that developed for GLC and is expressed in equation 24. Comparisons of the values of these thermodynamic properties can be indicative of the solubility of the polymer in a given solvent. Dincer and Bonner [1978] conclude that a high positive value of Δ , a highly negative value of χ , and similar solubility parameters for the polymer and solvent at 25°C indicates that the solvent will successfully dissolve the polymer.

Dangayach, Karim, and Bonner [1981] also use GSC to estimate the degree of polymer-solvent interaction of m-phenylene polybenzimidazole (PBI). The results of the interpretation of GSC data were further supported by quantitative solubility experiments. Further work in this area is certain to provide the necessary thermodynamic database for researchers and industry concerning polymer-solvent interactions.

In summary, inverse gas chromatography, either GLC or GSC, provides a means of investigating the thermodynamic interactions of a solute and a thermally stable polymer. Below T_g information is obtained about adsorption isotherms, as well as, solubility. Above T_g infinite dilution activity coefficients, diffusion constants, and solubility information are obtainable. The method is also valuable in studying the thermal transitions of a polymer. Since degradation of the stationary phase adversely affects the accuracy of the data, gas-solid chromatography is preferred when the polymer under consideration becomes thermally unstable above the glass transition temperature.

III. Experimental Protocol

In order that the method of inverse gas chromatography be applicable to the study of thermodynamic interactions of lignin and various solvents, preliminary thermal stability information was needed. The effect of polymer degradation at elevated temperatures during column preparation and prolonged use was extensively studied by Chang and Bonner [1975]. The polymer of interest was poly(ethylene oxide). They observed significant weight loss and discussed the impact this had on final results. Since the specific retention volume, V_g^0 , is calculated directly from the retention time, t_g , the effect of degradation will manifest itself two-fold. Firstly, lower retention times than expected for the presumed polymer loading will be obtained. Additionally, calculation of V_g^0 from t_g will be adversely affected due to its direct dependence on polymer loading, W_2 (see equation 12).

Differential Scanning Calorimetry (DSC) was used to investigate the glass transition temperature as well as the onset of thermal degradation. Weight loss data for the purpose of assessing thermal stability was also collected at a variety of temperatures.

Bench scale solubility studies were performed for comparative purposes. The data provided from these solubility studies will be used to qualitatively evaluate the reliability of the thermodynamic parameters

determined by inverse gas chromatography. Finally, a gas chromatograph is employed to investigate polymer-solvent interactions in which the stationary phase is a complex biopolymer, kraft lignin.

3.1. The Glass Transition Temperature and Thermal Stability of Lignin

Inverse gas chromatography can be performed at column temperatures above or below the glass transition temperature, T_g . Once a polymer has been chosen for study the researcher needs to accurately determine T_g . In addition, the tendency for the stationary phase to thermally degrade must be quantified to insure accurate data resulting from inverse gas chromatography.

3.1.1. Differential Scanning Calorimetry

The kraft lignin used in the work reported here was REAX® 27 kraft pine lignin manufactured by Westvaco. It has been reported by Glasser and coworkers [1984] that the glass transition temperature for kraft lignin lies near 170°C. To determine the glass transition temperatures of kraft lignin and HF lignin a differential scanning calorimeter was employed.

A Du Pont 990 Thermal Analyzer with a DSC cell base was used. Aluminum oxide was chosen to be the reference material. An estimate of T_g was made from the resulting thermograms and preliminary information concerning the thermal stability was obtained.

3.1.2. Isothermal Degradation Studies

As stated previously, if the polymer of interest shows thermal degradation at the temperatures employed in the inverse GC study it must be determined to what extent the degradation will occur. If the polymer is determined to be thermally unstable the information obtained from the chromatograms must be corrected during data analysis. Samples of both kraft lignin and HF lignin were weighed into tared sample pans and covered. All of the samples were dried to a constant weight at 110°C before testing at elevated temperatures. At 110°C no degradation of either kraft lignin or HF lignin was observed. The ovens used for the weight loss studies operate within $\pm 3^\circ\text{C}$ of the set point. The temperatures investigated ranged between 160°C and 250°C.

3.2. Solubility Studies

Solubility studies were performed in order to evaluate the ability of various solvents to dissolve or swell kraft lignin. Previous work by Schuerch [1952] indicates that the effectiveness of a solvent to dissolve various lignins increases as the hydrogen-bonding capacities of the solvents increase and as their Hildebrand solubility parameter (δ_1) approaches a value of eleven $(\text{cal/cc})^{1/2}$. The hydrogen-bonding capacity was determined to be proportional to the shift in wavelength ($\Delta\mu$) of the oxygen-deuterium band when a mixture of the solvent and heavy methanol (CH_3OD) were analyzed by infrared spectrometry [Gordy, 1941].

Glasser and coworkers [1984] assessed the solubility character of a variety of lignins and lignin derivatives with known absorptivity coefficients (A_{280}) at 280 nm. This was accomplished by adding 500 μ l of solvent to 100 mg dry lignin powder and shaking for 24 hours at room temperature. Undissolved solids were removed by filtration through glass wool and a 10 μ l aliquot was diluted to a 25 ml. The absorbance of UV light was determined for each solution at 280 nm.

The studies completed for this work were performed in the following manner. Kraft lignin samples weighing 0.10 grams were mixed with 10 ml of reagent grade solvent. After shaking for 24 hours at room temperature the samples were filtered to remove any undissolved solids and the liquid filtrate was collected in a tared weighing dish. The filtrate was then placed in a vacuum oven and dried until a constant weight was obtained. The final weight measurement was then used to calculate the percentage of lignin which had dissolved.

3.3. Inverse Gas Chromatography Apparatus

After reviewing the results of the thermal stability studies it was determined that the inverse gas chromatography experiments should be performed below the glass transition temperature. Two temperatures, 130°C and 160°C were chosen for the study. The preferred method of column preparation for this work was coating the polymer of interest on an inert support. Due to the low bulk density of lignin, coverage ratios for the work presented here were less than 10%. Columns with higher coverage ratios in the range of 15% to 25% were prepared but the

resulting particle size was so large that efficient and uniform packing was not possible. Columns were also prepared and tested in which the lignin was directly packed into the tubing to yield a homogeneous lignin stationary phase.

3.3.1. Experimental Apparatus

A Varian Aerograph Model 3700 gas chromatograph fitted with a flame ionization detector (FID) was employed for this work. A Matheson model 8L-580 regulator was used to maintain a constant flow rate of the carrier gas to minimize gas flow rate effects on the chromatograms. The column oven temperature was maintained within $\pm 1^\circ\text{C}$ of the setpoint. The flow rate of helium used as the carrier gas was measured at the column outlet by a soap-bubble flowmeter. Column inlet and outlet pressures were monitored within ± 0.5 mm Hg. The column outlet pressure was atmospheric pressure as measured barometrically. The solvents were injected through a silicone rubber septum using a $1\ \mu\text{l}$ Hamilton syringe. The plotting of chromatograms and determination of peak retention time was accomplished using a Hewlett-Packard model 3390A Reporting Integrator. A schematic of the gas chromatographic apparatus is shown in Figure 2.

3.3.2. Probe Molecules and Stationary Phases

Throughout this work 19 different solvents were used as probe molecules. The solvents used were reagent grade materials supplied by various manufacturers and were used with no further purification.

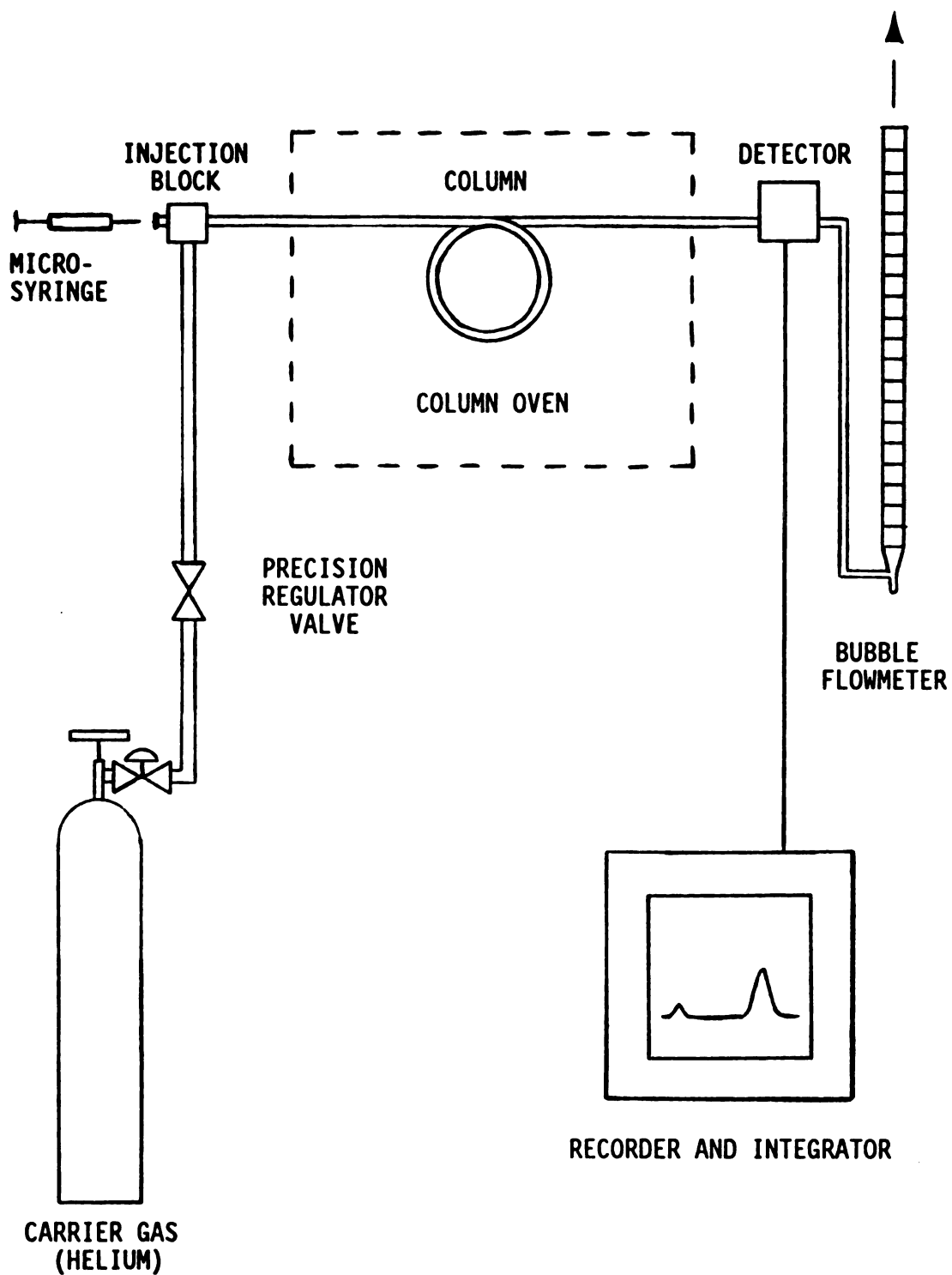


Figure 2. Schematic of Gas Chromatographic Apparatus

A powdered polytetrafluoroethylene was used as the inert support due to its reported ability to yield symmetric peaks independent of the polarity of the solvent [Newman and Prausnitz, 1972]. This implies that there is no interaction between the support and the probe molecules. Fluoropak 80® was supplied by Fluorocarbon Inc. of Anaheim, California. The specified mesh size was 60 microns to 70 microns.

The kraft pine lignin (REAX® 27) was supplied by Westvaco Chemicals of Charleston Heights, South Carolina. This grade of kraft lignin is insoluble at neutral and acidic pH. It is manufactured specifically for use in phenol formaldehyde resin systems. The HF lignin was obtained from liquid phase HF saccharification experiments performed at Michigan State University by Kevin Downey.

3.3.3. Column Preparation

The columns were prepared using 1/4 inch O.D. 26 B.W.G. gage stainless steel tubing. The length of the columns varied between 3.5 feet and 4.5 feet.

The columns were prepared in the following manner. A predetermined amount of lignin was dissolved in a suitable solvent (dimethylformamide was used for kraft lignin). A specific amount of the Fluoropak 80® was then added to the solution and the solvent removed by evaporation on a rotary evaporator. Dimethylformamide was readily removed at 70°C under 27 inches Hg vacuum. Once the mixture was reduced to a very thick slurry it was transferred to a large crystallizing dish. With the remaining

solvent just covering the solids the mixture was placed in a vacuum oven to complete the coating process. The packing was then dried for several days at 60°C. The packing was also heated overnight to 110°C under vacuum to obtain a steady weight. Upon removal from the oven it was noted that some of the particles had formed agglomerates. The aggregates were carefully separated so that exposure of the inert support surface was minimized. Next the packing material was sieved to remove any large particles and any fines resulting from separation of the larger agglomerates. The resulting particle size distribution was between 250 microns and 1000 microns. The particles were then inspected to eliminate those for which the coverage was not uniform or exposed support could be seen. Finally, the coverage ratio could be calculated based on the total weight of all particles resulting from the packing preparation process.

The stainless steel tubing used for the columns was cleaned and dried. Glass wool was used to prevent the packing from exiting the end of the column. The packing was then slowly added through a funnel to the column. A vibrating device was used to insure uniform packing throughout the length of the column. A glass wool plug was then used to maintain the packing within the column. The total amount of packing placed in the column was then recorded.

The ends of the column were fitted with 1/4 inch fittings and the column was coiled using a spring tube bender to fit in the chromatograph oven. Once the column was placed in the oven it was conditioned by heating to 170°C, 10°C above the maximum operating temperature used in this study, with a steady flow of carrier gas through it. No degradation products

were detected by the FID during the conditioning for any of the columns used.

Two kraft lignin columns were prepared; 8.4% coverage ratio and 3.96% coverage ratio. The total amount of packing in the columns varied between 17 and 18 grams. Preparation of HF lignin column packings was complicated due to the strong adhesive properties of this material. A tacky film would result on top of the inert support and attempts to separate the agglomerates were unsuccessful. Several attempts to prepare a suitable packing had similar results. For these reasons, it was decided that the analysis would be performed exclusively using kraft lignin. Particular attention would be paid to column loading and temperature effects.

3.3.4. Experimental Procedure

The carrier gas flow rate was set between 8 and 11 ml/min as determined at room temperature before each series of injections. Flow rates obtained below this level were found difficult to control. Since an essentially negligible difference between the retention volume obtained by extrapolation to zero flow rate and the retention volume at the above flow rates was observed, rates between 8 and 11 ml/min were taken to approximate zero flow rate conditions. It should also be noted that one of the goals of this work is to demonstrate that inverse gas chromatography provides a rapid method of investigating lignin-solvent interactions, therefore, it is not practical to operate at very low flow rates.

It was necessary to select an appropriate reference for the flame ionization detector. As will be seen in the data analysis section it is required that the compound be a member of a specific class of "simple" compounds (ie. normal alkanes, normal alcohols, etc.) and exhibit little or no interaction with the polymer under investigation. For this work ethane was chosen as the reference material. It was obtained from a small lecture cylinder using a gas-tight syringe. Experimental data showed that the specific retention volume of ethane was independent of both sample size and carrier gas flow rate in the range of 8 to 11 ml/min.

A Hamilton 1 μ l gas-tight syringe was used to inject solvent through a silicone rubber septum at the injection port. Sample size was varied between "residual" solvent and 0.2 μ l. "Residual" solvent injections were accomplished by flushing the syringe several times with the solvent then 0.1 μ l of liquid was drawn in and flushed out. Finally, 0.1 μ l of the residual solvent was injected into the chromatograph and the response recorded. It was found for all the solvents tested that retention data was independent of sample size within this range. At the same time symmetric peaks were obtained for these injections. In order that easily detectable peaks could be recorded, 0.1 μ l was chosen as the sample size.

As was previously discussed in the review of the development of inverse gas chromatography, symmetric peaks do not guarantee that adsorption of the solute on the polymer and support is not occurring [Conder, 1971]. It was noted by Newman and Prausnitz [1972] that coverage ratios greater than 15% provided consistent, as well as, accurate results. In the case

of the work described here coverage ratios of this magnitude were not obtainable due to particle size restrictions on the packing. It was, therefore, necessary to demonstrate that adsorption on the support would not occur if any exposed surface resulted during the coating process. This was accomplished by packing a column of the same dimensions with pure Fluoropak 80® and injecting several solvents under similar operating conditions and recording retention data. It was found that, independent of sample size, all solvents including the reference, ethane, had the same retention time. This serves to verify that no interaction is occurring between the solid support and the probe molecule. Secondly, it once again confirms the observation made by several researchers that Fluoropak 80® is the support of choice for inverse gas chromatography applications.

Retention time measurements were made using the Hewlett-Packard Reporting Integrator. Determination of the peak retention time or peak apex was achieved in the following manner. Once the start of a peak has been recognized and confirmed the slopes of successive peak segments are evaluated. The size of the peak segments can be controlled manually. When three successive peak segments show a downslope the integrator begins a quadratic fit to establish the apex. The mathematical fit utilizes the values of the peak height for the maximum segment, the segment immediately before the maximum segment, and the segment analyzed immediately after the maximum segment.

IV. Discussion of Results

4.1. Determination of T_g and Thermal Stability

Typical thermograms for both kraft lignin and HF lignin are depicted in Figure 3. The glass transition temperature is represented by an exotherm on the thermal trace. The initial dip in the thermogram represents the endothermic vaporization of water from the sample. The glass transition temperature of kraft lignin is shown to be at the inflection point on the thermogram which corresponds to 178°C. Above 200°C it appears that kraft lignin begins to decompose. By comparison, the thermal trace for HF lignin does not contain an inflection point identifying the glass transition temperature. The sharp upward endotherm on the thermogram implies that this form of lignin decomposes at a temperature equal to, or greater than, T_g . From the tracing it can be concluded that T_g exceeds 180°C, where endothermic decomposition proceeds at a rapid rate.

Table 2 summarizes the results of the thermal stability study as the percent weight lost at a given temperature. Two samples were tested at each of the temperatures and the results were considered reproducible if less than 3% variability was observed. The samples were subjected to the oven temperature until the weight loss varied less than 1% of the initial sample weight, about 20 hours.

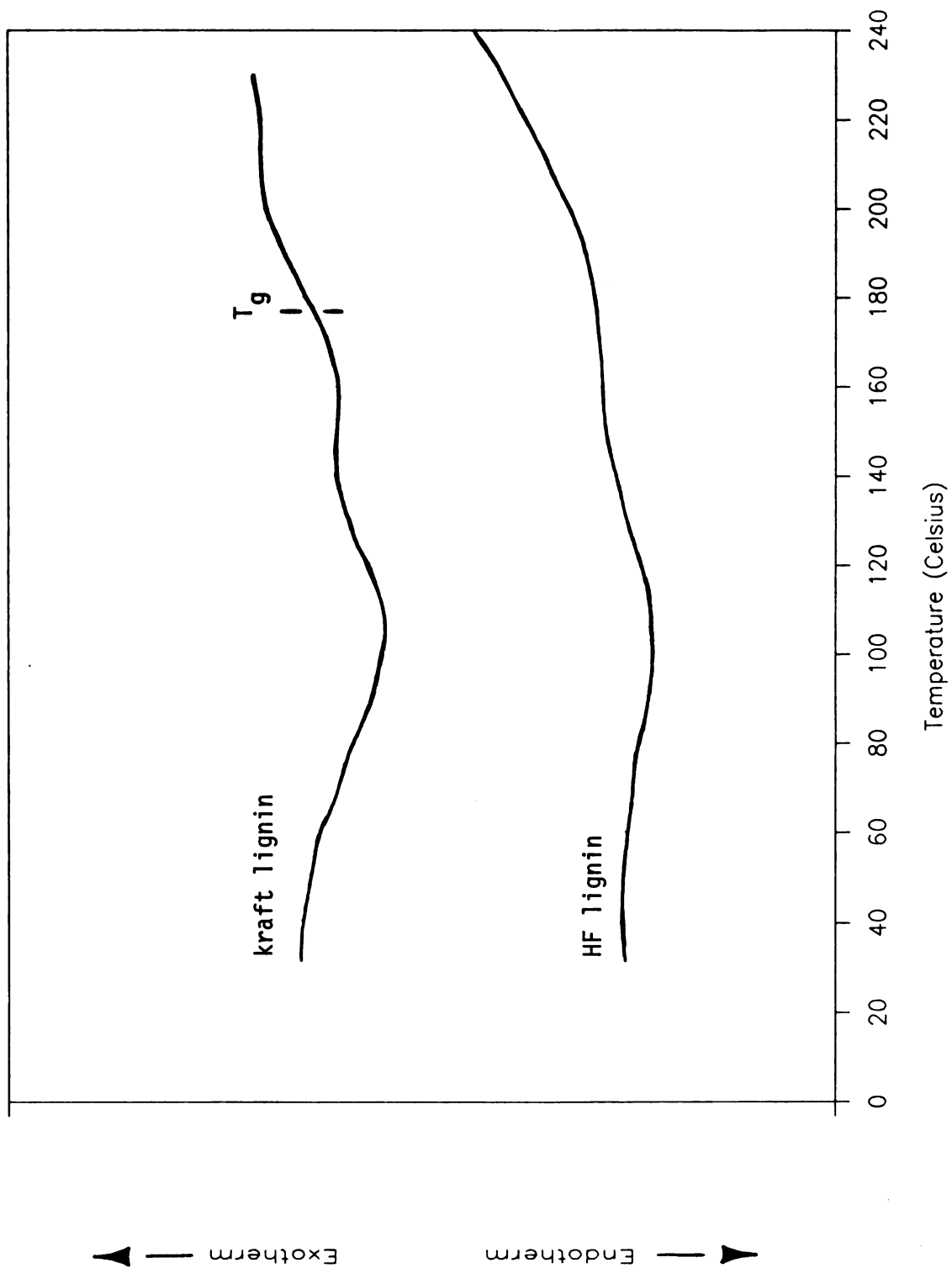


Figure 3. Differential Scanning Calorimetry Traces

Table 2. Results of Isothermal Weight Loss Study

<u>Testing Temperature (°C)</u>	<u>Percent Weight Lost</u>	
	<u>Kraft Lignin</u>	<u>HF Lignin</u>
160	5%	9%
175	7%	14%
200	8%	23%
225	15%	50%
250	23%	55%

It can be seen from the data in Table 2 that the weight loss data supports the information obtained from the DSC thermograms. HF lignin decomposes rapidly at temperatures exceeding 150°C. This may be an indication that carbon-carbon bonds formed by auto-condensation during the saccharification process are subject to weakening at elevated temperatures. At temperatures greater than 200°C these bonds break and result in decomposition of the lignin. On the other hand, kraft lignin is shown to be relatively stable until exposed to temperatures above 200°C.

It is clearly evident that for meaningful data to be collected from inverse gas chromatograms polymer losses due to thermal instability must be minimized. For this reason column operating temperatures were chosen to be less than the glass transition temperature. The two temperatures chosen for the study of lignin-solvent interactions were 130°C and 160°C. Table 2 shows that it is expected that kraft lignin will undergo less than or equal to a 5% weight change due to thermal decomposition over extended periods of time. This indicates that once the column is

conditioned at these temperatures there should be no change in polymer loading.

4.2. Solubility Studies

Solvents determined by Schuerch to afford homogenous solutions for kraft "Indulin" lignin® at a concentration of 0.1 gram lignin per 10 ml solvent are listed in Table 3 along with their corresponding solubility parameter and $\Delta\mu$ value.

Table 3. Effective Solvents for Kraft "Indulin" Lignin [Schuerch, 1952].

<u>Solvent</u>	<u>$\Delta\mu$</u>	<u>$\delta_1^{1/2}$ (cal/cc)^{1/2}</u>
Diethylene glycol	high	9.1
Dioxane	0.14	10.0
Pyridine	0.27	10.7
Methyl cellosolve	high	10.8
Ethylene glycol	0.31	14.2

The solubility results of Glasser and coworkers [1984] for kraft "Indulin AT"® lignin are summarized in Table 4. Their analysis leads to results in terms of weight percent (ie. mg/ml).

The results of the bench scale solubility studies for kraft lignin are summarized in Table 5. The results are reported as weight percent (%) of lignin soluble and the solubility parameters are included for comparison.

Table 4. Results of Solubility Studies by Glasser and coworkers for Kraft lignin ^a [Glasser et al, 1984].

<u>Solvent</u>	<u>δ_1 (cal/cc)^{1/2}</u>	<u>Wt. % Soluble</u>
Methanol	14.51	13
Dimethylformamide	11.80	>20
Dioxane	11.80	>20
90% Aqueous dioxane		>20
2-Butanone	9.30	18
Acetonitrile	11.90	4
Tetrahydrofuran	12.10	>20
Chloroform	9.30	14

^a Absorptivity coefficient for kraft "Indulin AT"® lignin, $A_{280} = 20.3$ g/l/cm.

The only solvent which completely dissolved the lignin at a concentration of 10 mg/ml was dimethylformamide with a solubility parameter of 11.8 (cal/cc)^{1/2}. Methyl cellosolve and dioxane successfully dissolved greater than 5 mg/ml of lignin.

There are some comparisons to be made between the various sources of solubility data. In particular, Glasser and coworkers determine a much higher solubility of kraft lignin in methanol, dioxane, and chloroform. Both types of kraft lignin are the result of a kraft pine pulping process. Kraft "Indulin AT"® is isolated for use in a variety of minor applications, whereas, kraft REAX® 27 is specifically designed for use as a co-reactant in phenol formaldehyde resin systems. As noted previously, lignin may undergo auto-condensation reactions even when conditions are

Table 5. Results of Bench Scale Solubility Studies for Kraft REAX 27 Lignin

<u>Solvent</u>	<u>δ_1 (cal/cc)^{1/2}</u>	<u>Weight Percent Lignin Soluble</u>
Dimethylformamide	11.80	>10.0
Methyl Cellosolve	10.80	9.82
Dioxane	10.00	7.82
Methanol	14.51	4.99
Acetone	10.00	3.58
Ethanol	12.90	1.77
Methyl ethyl ketone	9.30	1.39
Acrylonitrile	11.00	0.95
Diethyl ether	7.40	0.64
Ethyl acetate	9.10	0.54
Chloroform	9.30	0.54
Benzene	9.15	0.46
Chlorobenzene	9.50	0.41
Toluene	8.90	0.36
Carbon tetrachloride	8.60	0.35
n-Propanol	12.05	0.20
n-Butanol	11.40	0.05
i-Propanol	11.60	0.04

mild. The isolation conditions used to obtain these two grades of lignin vary and result in differing physical properties for each form. The differences in solubility between these two types of lignin have been observed by the manufacturer [Roberts, 1987].

4.3. Inverse Gas Chromatography

4.3.1. Specific Retention Volume

The calculated values of specific retention volume for kraft lignin are shown in Tables 6 through 9. Equation 12 describes the relationship between experimental data and the specific retention volume. The data in Tables 6 through 9 were collected on two columns with different loadings at two different operating temperatures. The carrier gas flow rate is corrected for the appropriate column operating temperature. The quantity f_p represents the correction to the specific retention volume due to pressure drop across the column (see equation 13). Retention times t_r and t_g represent those for the reference gas, ethane, and solvent, respectively.

4.3.2. Physical Properties of Solvents and Calculation of the Flory-Huggins Interaction Parameter

The models proposed by Dangayach and coworkers [1981] for the molar Gibbs energy of adsorption, as well as, the correlation for the Flory-Huggins interaction parameter require the use of several pure solvent properties. Among these are liquid molar volumes, saturated vapor pressures, second virial coefficients, polarizabilities, and dipole moments. Not all of

Table 6. Specific Retention Volume Calculations for 8.4% Coverage of Kraft Lignin at 130°C ($m_2 = 1.511$ g).

Solvent	Carrier Gas Flow Rate (Q, cc/min)	f_p	Retention Times		Specific Retention Volume (V_g^0 , cc/g)
			t_r (min)	t_g (min)	
Dioxane	12.22	0.956	0.85	1.23	1.99
Methanol	13.25	0.956	0.85	2.09	7.04
Acetone	12.22	0.956	0.85	1.41	2.93
Ethanol	12.22	0.956	0.85	1.64	4.14
Methyl ethyl ketone	13.25	0.956	0.85	1.32	2.67
Acrylonitrile	12.22	0.956	0.85	2.67	9.53
Diethyl ether	13.25	0.956	0.85	0.88	0.170
Ethyl acetate	13.25	0.956	0.85	1.09	1.36
Chloroform	13.25	0.956	0.85	1.03	1.02
Benzene	12.22	0.956	0.85	1.10	1.31
Chlorobenzene	12.22	0.956	0.85	2.32	7.70
Toluene	12.22	0.956	0.85	1.27	2.20
Carbon tetrachloride	13.25	0.956	0.85	0.88	0.170
n-Propanol	12.22	0.956	0.85	1.39	2.83
n-Butanol	12.22	0.956	0.85	1.43	3.04
i-Propanol	13.25	0.956	0.85	0.91	0.341

Table 7. Specific Retention Volume Calculations for 8.4% Coverage of Kraft Lignin at 160°C ($m_2 = 1.511$ g).

Solvent	Carrier Gas Flow Rate (Q, cc/min)	f_p	Retention Times		Specific Retention Volume (V_g^0 , cc/g)
			t_r (min)	t_g (min)	
Dioxane	12.87	0.940	0.78	1.13	1.77
Methanol	12.87	0.940	0.78	1.20	2.12
Acetone	12.87	0.940	0.78	1.04	1.31
Ethanol	12.87	0.940	0.78	1.09	1.56
Methyl ethyl ketone	12.87	0.940	0.78	1.06	1.41
Acrylonitrile	12.87	0.940	0.78	1.40	3.13
Diethyl ether	12.87	0.940	0.78	0.84	0.303
Ethyl acetate	12.87	0.940	0.78	0.93	0.757
Chloroform	12.87	0.940	0.78	0.92	0.707
Benzene	12.87	0.940	0.78	1.00	1.11
Chlorobenzene	12.87	0.940	0.78	1.56	3.94
Toluene	12.87	0.940	0.78	1.08	1.51
Carbon tetrachloride	12.87	0.940	0.78	0.83	0.252
n-Propanol	12.87	0.940	0.78	1.06	1.41
n-Butanol	12.87	0.940	0.78	1.13	1.77
i-Propanol	12.87	0.940	0.78	0.88	0.505

Table 8. Specific Retention Volume Calculations for 3.96% Coverage of Kraft Lignin at 130°C ($m_2 = 0.697$ g).

Solvent	Carrier Gas Flow Rate (Q, cc/min)	f_p	Retention Times		Specific Retention Volume (V_g^0 , cc/g)
			t_r (min)	t_g (min)	
Dioxane	14.72	0.855	0.79	1.32	6.48
Methanol	14.44	0.872	0.79	1.62	10.2
Acetone	14.72	0.855	0.79	1.40	7.46
Ethanol	14.72	0.855	0.79	1.48	8.44
Methyl ethyl ketone	14.44	0.872	0.79	1.51	8.81
Acrylonitrile	14.72	0.855	0.79	2.37	19.3
Diethyl ether	14.44	0.872	0.79	0.85	0.734
Ethyl acetate	14.44	0.872	0.79	1.21	5.14
Chloroform	14.44	0.872	0.79	1.04	3.06
Benzene	14.72	0.855	0.79	1.09	3.67
Chlorobenzene	14.72	0.855	0.79	2.80	24.6
Toluene	14.72	0.855	0.79	1.30	6.24
Carbon tetrachloride	14.44	0.872	0.79	0.88	1.10
n-Propanol	14.72	0.855	0.79	1.48	8.44
n-Butanol	14.72	0.855	0.79	1.67	10.8
i-Propanol	14.44	0.872	0.79	0.95	1.96

Table 9. Specific Retention Volume Calculations for 3.96% Coverage of Kraft Lignin at 160°C ($m_2 = 0.697$ g).

Solvent	Carrier Gas Flow Rate (Q, cc/min)	f_p	Retention Times		Specific Retention Volume (V_g^0 , cc/g)
			t_r (min)	t_g (min)	
Dimethylformamide	62.02	0.652	0.17	1.91	63.7
Dioxane	15.77	0.852	0.73	1.10	4.50
Methanol	15.77	0.852	0.73	0.98	3.04
Acetone	15.77	0.852	0.73	0.99	3.16
Ethanol	15.77	0.852	0.73	1.00	3.28
Methyl ethyl ketone	15.77	0.852	0.73	1.02	3.53
Acrylonitrile	15.77	0.852	0.73	1.27	6.56
Diethyl ether	15.77	0.852	0.73	0.75	0.243
Ethyl acetate	15.77	0.852	0.73	0.89	1.94
Chloroform	15.77	0.852	0.73	0.86	1.58
Benzene	15.77	0.852	0.73	0.82	1.09
Chlorobenzene	15.77	0.852	0.73	1.57	10.2
Toluene	15.77	0.852	0.73	0.95	2.67
Carbon tetrachloride	15.77	0.852	0.73	0.76	0.365
n-Propanol	15.77	0.852	0.73	1.01	3.40
n-Butanol	15.77	0.852	0.73	1.13	4.86
i-Propanol	15.77	0.852	0.73	0.81	0.972

these parameters are readily available and, in many cases, it was necessary to calculate these quantities from appropriate correlations.

Many of the general properties of the solvent such as boiling point, critical properties, acentric factors (ω), and dipole moment were obtained from an extensive compilation contained in The Properties of Gases and Liquids [Reid et al, 1977]. Acentric factors, if not found in the previously mentioned reference, were calculated using a simple relation proposed by Edmister [Reid et al, 1977]. Dipole moments for compounds could be calculated, if necessary, using an empirical correlation based on an extended corresponding states theory developed by O'Connell and Prausnitz [1967]. Solvent polarizabilities were available from data reported in the National Bureau of Standard Circular by Maryott and Buckley [1953]. Since the temperature dependence of polarizability and dipole moment is not completely understood the values at 25°C were assumed to be constant; independent of column operating temperature. The general pure solvent properties can be found in Table 10.

In many cases values of the solvent molar volume and vapor pressure were available in Timmermans', Physico-Chemical Constants of Binary Systems [Timmermans, 1959]. Very accurate correlations for a few of the compounds were available in a collection of physical properties for industrially important compounds by Carl Yaws [1977]. When the necessary quantities were not available from either of the above two sources less rigorous methods were used. For liquid molar volumes a method developed by Gunn and Yamada was utilized [Reid et al, 1977]. The technique is derived from the theory of corresponding states. The method requires

Table 10. General Pure Solvent Properties

Solvent	T_b (°C)	T_c (°C)	P_c (atm)	MW	μ	ω	α_1 $\times 10^{24}$ (cc)	μ_1 $\times 10^{30}$ (C m)
DMF	153.0	323.7	46.48	73.09	3.82	0.7458	7.84	11.34
Dioxane	101.4	313.9	51.40	88.11	0.40	0.2880	8.56	1.40
Methanol	64.52	240.0	78.50	32.04	1.70	0.5556	3.25	5.67
Acetone	56.20	236.3	47.20	58.08	2.90	0.3035	6.43	9.61
Ethanol	78.35	243.1	62.96	46.07	1.70	0.6341	5.07	5.67
MEK	79.60	262.3	41.03	72.11	3.30	0.3188	8.24	9.24
Acrylonitrile	77.29	246.0	34.90	53.06	3.50	0.3853	6.19	12.77
Diethyl ether	34.60	193.6	35.61	74.12	1.30	0.2800	8.80	3.84
Ethyl acetate	77.10	250.1	38.00	88.10	1.90	0.3718	8.33	5.93
Chloroform	61.20	263.4	54.00	119.4	1.10	0.2117	8.32	3.40
Benzene	80.10	288.5	47.90	78.11	0.00	0.2116	10.40	0.00
Chlorobenzene	131.7	359.2	44.64	112.6	1.60	0.2545	12.34	5.70
Toluene	110.7	320.0	40.00	92.14	0.40	0.2415	12.34	1.23
CCl ₄	76.75	283.2	44.98	153.8	0.00	0.1938	10.24	0.00
n-Propanol	97.24	263.7	50.16	60.10	1.70	0.6111	6.90	5.64
n-Butanol	117.7	289.7	43.58	74.12	1.80	0.5903	8.76	5.57
i-Propanol	82.29	235.2	47.02	60.10	1.70	0.6614	6.94	5.34

References:

Maryott and Buckley, 1953

O'Connell and Prausnitz, 1967

Reid et al, 1977

knowledge of critical properties, the acentric factor, and a value of the saturated-liquid molar volume at any temperature. Saturated vapor pressures, on the other hand, were readily calculated from Antoine's equation using Antoine constants obtained from an appropriate source [Reid et al, 1977]. Table 11 lists liquid molar volumes and saturated vapor pressures obtained from the above references for the solvents studied.

Estimation of second virial coefficients was accomplished using several sources and methods. Constantine Tsonopoulos [1974] developed an empirical correlation useful for both polar and non-polar systems. He introduces a modification of the very successful Pitzer-Curl correlation initially proposed in 1957 [Pitzer and Curl, 1957]. Modelling of second virial coefficients is accomplished using reduced temperature, reduced dipole moment and the acentric factor. In cases where the constants for the Tsonopoulos correlation could not be accurately estimated the original Pitzer-Curl theory based on a three-parameter theory of corresponding states was applied [O'Connell and Prausnitz, 1967]. Some data was already available from previous inverse GLC work completed by Newman and Prausnitz [1973]. The second virial coefficients and the method used to obtain them are contained in Table 12.

Equation 24, which relates the specific retention volume to the Flory-Huggins interaction parameter, requires a value of the specific volume of the polymer, v_2 . This quantity was determined experimentally using a pycnometer. A measured weight of lignin was placed in the calibrated pycnometer. Water at 25°C was added to fill the pycnometer and the total

Table 11. Solvent Molar Volumes and Vapor Pressures

Solvent	Temperature 130°C		Temperature 160°C	
	V_1^* (cc/gmole)	P_1^{S*} (atm)	V_1^* (cc/gmole)	P_1^{S*} (atm)
Dimethylformamide	89.19 ^b	0.525 ^c	93.59 ^b	1.21 ^c
Dioxane	97.63 ^b	2.22 ^c	102.2 ^b	4.49 ^c
Methanol	47.33	8.21	50.54	17.1
Acetone	88.56 ^b	7.58 ^c	96.46 ^b	13.9 ^c
Ethanol	67.86	5.68	72.79	12.3
Methyl ethyl ketone	105.6 ^b	4.09 ^c	114.6 ^b	7.87 ^c
Acrylonitrile	78.79 ^b	3.87 ^c	85.72 ^b	7.20 ^c
Diethyl ether	132.8	12.05	149.8	20.8
Ethyl acetate	117.0	4.34	125.3	8.38
Chloroform	95.08 ^a	6.34 ^a	101.2 ^a	11.6 ^a
Benzene	103.2	3.71	108.7	6.97
Chlorobenzene	114.4	0.946	118.7	2.02
Toluene	121.7 ^a	1.67	127.5 ^a	3.85
Carbon tetrachloride	112.4	3.95	118.5	7.29
n-Propanol	85.91	3.02	91.05	6.93
n-Butanol	106.3 ^a	1.51 ^a	112.5 ^a	3.64 ^a
i-Propanol	93.14 ^b	4.94 ^c	101.9 ^b	10.9 ^c

* Data were obtained from Timmermans, 1959, unless otherwise indicated.

^a Source: Yaws, 1977.

^b Source: Gunn and Yamada technique [Reid et al, 1977].

^c Source: Antoine's Equation [Reid et al, 1977].

Table 12. Second Virial Coefficients

Solvent	μ_r	Constants		B_{11} (cc/gmole)	
		a	b	130°C	160°C
Dimethylformamide ³	190.4			1970	1610
Dioxane ³	2.39			826	660
Methanol ¹	6.15	.0878	.0560	388	296
Acetone ¹	153.0	-.03133	0	659	531
Ethanol ¹	68.27	.0878	.05657	520	393
Methyl ethyl ketone ¹	155.9	-.03192	0	944	752
Acrylonitrile ¹	158.6	-.03567	0	1024	812
Diethyl ether ¹	27.62	.00344	0	539	452
Ethyl acetate ²	50.10			812	651
Chloroform ²	22.70			521	441
Benzene ¹	0			714	601
Chlorobenzene ³	28.58			1390	1024
Toluene ¹	1.82	0	0	1025	854
Carbon tetrachloride ¹	0			727	602
n-Propanol ¹	50.29	.0878	.04406	687	528
n-Butanol ¹	44.57	.0878	.04009	939	712
i-Propanol ¹	52.59	.0878	.0537	684	485

¹ Tsonopoulos correlation [Tsonopoulos, 1974].

² Pitzer-Curl correlation [O'Connell and Prausnitz, 1967].

³ Source: Newman and Prausnitz, October, 1973.

weight measured. Using the known density of water at 25°C, the specific volume of the polymer could be calculated. The specific volume for kraft lignin was found to be 1.538 cc/g.

Simplification of equation 20 can be accomplished by demonstrating that the quantity $V_1/(M_2V_2)$ will be sufficiently small that it can be assumed to be negligible. Glasser and coworkers have determined the average molecular weight ($M_w \approx M_2$) of kraft "Indulin AT"® lignin to be approximately 44,000 [Glasser et al, 1984]. If this value is assumed to be approximately that of the lignin used here, one finds that $V_1/(M_2V_2) \approx 0.002$ for diethyl ether at 160°C (ie. the largest value of V_1 in this study). Since this represents a very small contribution to χ it will be neglected. The values of the Flory-Huggins interaction parameters calculated using equation 24 are located in Tables 13 through 16.

4.3.3. Specific Interaction Parameter Data Analysis

As was previously mentioned, the models proposed by Dangayach and coworkers can be used to identify various types of intermolecular forces which may occur between the solvent and polymer. Combining this analysis with values for the interaction parameter and the solubility parameter can allow one to draw conclusions regarding the ability of a particular solvent to swell or dissolve a polymer. The following paragraphs outline the mathematical analysis used to determine the specific interaction parameter, Δ .

Table 13. Data Analysis for 8.4% Coverage at 130°C

<u>Solvent</u>	<u>v_g^0 (cc/g)</u>	<u>χ</u>	<u>ΔG_{ads}</u>	<u>ΔG_{ad} (kJ/gmole)</u>	<u>ΔG_{ads}^*</u>	<u>Λ (kJ/gmole)</u>
2 Dioxane	1.99	3.33	-16.3	5.74	-21.2	4.87
3 Methanol	7.04	1.45	-15.4	4.89	-16.7	1.33
4 Acetone	2.93	1.73	-16.4	4.94	-15.3	-1.09
5 Ethanol	4.14	1.99	-16.0	4.89	-17.3	1.33
6 Methyl ethyl ketone	2.67	2.29	-16.0	5.94	-16.1	0.129
7 Acrylonitrile	9.53	1.36	-12.7	8.56	-13.2	0.533
8 Diethyl ether	.170	3.69	-25.1	-2.98	-19.7	-5.38
9 Ethyl acetate	1.36	2.82	-17.5	4.47	-18.2	0.740
10 Chloroform	1.02	2.94	-17.5	4.46	-19.8	2.33
11 Benzene	1.31	3.16	-18.1	0	-18.1	0
12 Chlorobenzene	7.70	2.69	-10.9	7.84	-15.2	4.25
13 Toluene	2.20	3.30	-15.8	2.94	-18.0	2.17
14 Carbon tetrachloride	.170	5.05	-22.6	0	-22.6	0
15 n-Propanol	2.83	2.80	-16.4	5.09	-18.0	1.55
16 n-Butanol	3.04	3.22	-15.4	6.71	-18.6	3.20
17 i-Propanol	.341	4.30	-23.5	-1.99	-18.2	-5.34

Table 14. Data Analysis for 8.4% Coverage at 160°C

<u>Solvent</u>	<u>v_g^0 (cc/g)</u>	<u>χ</u>	<u>ΔG_{ads}</u>	<u>ΔG_{ad} (kJ/gmole)</u>	<u>ΔG_{ads}^*</u>	<u>Λ (kJ/gmole)</u>
2 Dioxane	1.77	2.68	-17.9	5.18	-22.5	4.63
3 Methanol	2.12	1.81	-20.9	2.77	-21.4	0.526
4 Acetone	1.31	1.80	-20.5	2.82	-19.5	-0.98
5 Ethanol	1.56	2.09	-20.7	2.77	-21.2	0.526
6 Methyl ethyl ketone	1.41	2.16	-19.4	3.72	-19.5	0.066
7 Acrylonitrile	3.13	1.73	-17.7	5.65	-18.3	0.595
8 Diethyl ether	.303	2.42	-24.9	-1.84	-21.5	-3.36
9 Ethyl acetate	.757	2.65	-21.0	2.11	-20.8	-0.24
10 Chloroform	.707	2.61	-20.1	3.01	-21.8	1.67
11 Benzene	1.11	2.62	-20.0	0	-20.0	0
12 Chlorobenzene	3.94	2.55	-14.1	5.69	-17.5	3.43
13 Toluene	1.51	2.76	-18.3	1.49	-19.3	1.00
14 Carbon tetrachloride	.252	3.97	-22.9	0	-22.9	0
15 n-Propanol	1.41	2.57	-20.1	3.17	-21.0	0.937
16 n-Butanol	1.77	2.80	-18.5	4.56	-20.9	2.36
17 i-Propanol	.505	3.01	-23.8	-0.54	-21.1	-2.65

Table 15. Data Analysis for 3.96% Coverage at 130°C

Solvent	v_g^0 (cc/g)	χ	ΔG_{ads}	ΔG_{ad}	ΔG_{ads}^*	Λ
				(kJ/gmole)		(kJ/gmole)
2 Dioxane	6.48	2.15	-12.3	4.65	-16.2	3.89
3 Methanol	10.2	1.08	-14.2	4.50	-15.6	1.40
4 Acetone	7.46	.800	-13.2	4.46	-12.4	-0.80
5 Ethanol	8.44	1.28	-13.6	4.50	-15.0	1.40
6 Methyl ethyl ketone	8.81	1.10	-11.9	5.16	-12.0	0.098
7 Acrylonitrile	19.3	.655	-10.3	7.44	-10.7	0.441
8 Diethyl ether	.734	2.23	-20.2	-3.33	-14.8	-5.42
9 Ethyl acetate	5.14	1.49	-13.1	3.93	-13.8	0.681
10 Chloroform	3.06	1.85	-13.8	3.23	-15.2	1.37
11 Benzene	3.67	2.13	-14.6	0	-14.6	0
12 Chlorobenzene	24.6	1.52	-7.01	6.95	-10.8	3.83
13 Toluene	6.24	2.26	-12.3	1.66	-13.3	0.986
14 Carbon tetrachloride	1.10	3.18	-16.4	0	-16.4	0
15 n-Propanol	8.44	1.70	-12.7	4.80	-14.4	1.71
16 n-Butanol	10.8	1.95	-11.2	5.69	-13.8	2.64
17 i-Propanol	1.96	2.56	-17.6	-0.11	-14.6	-3.03

Table 16. Data Analysis for 3.96% Coverage at 160°C

Solvent	v_g^0 (cc/g)	χ	ΔG_{ads}	ΔG_{ad} (kJ/gmole)	ΔG_{ads}^*	Λ (kJ/gmole)
1 Dimethylformamide	63.7	.513	-5.66	18.1	-14.7	9.01
2 Dioxane	4.50	1.74	-14.5	8.58	-22.0	7.46
3 Methanol	3.04	1.45	-19.6	8.15	-23.2	3.62
4 Acetone	3.16	.925	-17.3	7.65	-17.3	-0.01
5 Ethanol	3.28	1.35	-18.0	8.15	-21.6	3.62
6 Methyl ethyl ketone	3.53	1.24	-16.1	7.26	-16.0	-0.01
7 Acrylonitrile	6.56	.994	-15.0	10.2	-15.0	-0.02
8 Diethyl ether	.243	2.64	-25.7	-2.83	-19.8	-5.89
9 Ethyl acetate	1.94	1.70	-17.6	5.68	-18.6	0.951
10 Chloroform	1.58	1.81	-17.2	6.09	-20.6	3.34
11 Benzene	1.09	2.63	-20.1	0	-20.1	0
12 Chlorobenzene	10.2	1.59	-10.7	7.69	-13.9	3.15
13 Toluene	2.67	2.19	-16.3	2.09	-17.4	1.11
14 Carbon tetrachloride	.365	3.60	-21.6	0	-21.6	0
15 n-Propanol	3.40	1.69	-16.9	7.64	-20.0	3.14
16 n-Butanol	4.86	1.79	-14.9	8.00	-18.5	3.56
17 i-Propanol	.972	2.35	-21.4	3.10	-20.2	-1.15

The molar Gibbs energy of adsorption, ΔG_{ads} , is calculated from the specific retention volume using equation 44. It is then necessary to fit ΔG_{ads} according to the model in equation 45. A plot of ΔG_{ads} versus polarizability, α_1 , is prepared for each of the operating temperatures and column loadings (see Figures 4 through 7). Two of the primary alcohols, methanol and ethanol, have the same dipole moment. We would expect that the specific interactions of each of these compounds with kraft lignin are similar. Since the last three contributions in the model in equation 44 will be constant for these two compounds we can determine the constant a by drawing a straight line through these two data points.

Once the constant a has been determined it becomes necessary to determine the constant, c . The dipole moments for carbon tetrachloride and benzene are equal to zero, therefore, the constant c can be determined by assuming Δ equal to zero for each of these compounds. If a straight line with slope a is drawn through both carbon tetrachloride and benzene we can use equation 45 to determine the constant c_1 and c_2 . The lines represented by $(\alpha_1 + c_1)$ and $(\alpha_1 + c_2)$ in Figures 4 through 7 are referred to as the reference lines for aliphatic and aromatic compounds, respectively. The equations describing the aliphatic reference lines for each data set are:

$$\Delta G_{ads} (130^\circ\text{C}, 8.4\% \text{ cvg.}) = -3.30 \times 10^{23} \alpha_1 - 19.2 \quad (46)$$

$$\Delta G_{ads} (160^\circ\text{C}, 8.4\% \text{ cvg.}) = 1.10 \times 10^{23} \alpha_1 - 24.0 \quad (47)$$

$$\Delta G_{ads} (130^{\circ}\text{C}, 3.96\% \text{ cvg.}) = 3.30 \times 10^{23} \alpha_1 - 19.9 \quad (48)$$

$$\Delta G_{ads} (160^{\circ}\text{C}, 3.96\% \text{ cvg.}) = 8.79 \times 10^{23} \alpha_1 - 30.6 \quad (49)$$

The reference lines for aromatics are as follows:

$$\Delta G_{ads} (130^{\circ}\text{C}, 8.4\% \text{ cvg.}) = -3.30 \times 10^{23} \alpha_1 - 14.7 \quad (50)$$

$$\Delta G_{ads} (160^{\circ}\text{C}, 8.4\% \text{ cvg.}) = 1.10 \times 10^{23} \alpha_1 - 21.1 \quad (51)$$

$$\Delta G_{ads} (130^{\circ}\text{C}, 3.96\% \text{ cvg.}) = 3.30 \times 10^{23} \alpha_1 - 18.0 \quad (52)$$

$$\Delta G_{ads} (160^{\circ}\text{C}, 3.96\% \text{ cvg.}) = 8.79 \times 10^{23} \alpha_1 - 29.2 \quad (53)$$

The difference between the values of ΔG_{ads} predicted from the above equations and those determined experimentally is designated ΔG_{ad} . The quantity ΔG_{ad} represents interactions due to forces other than induced-dipole moments. The values of ΔG_{ad} are included in Tables 13 through 16 and are plotted versus the dipole moment, μ_1 in Figures 8 through 11. A reference line on these figures can be drawn through those points which represent solvents known not to form hydrogen bonds and which do not have charge transfer characteristics. Solvents such as acetone, methyl ethyl ketone, acrylonitrile and toluene provide the necessary data points.

Although chlorobenzene does not form hydrogen bonds, its peaks were not very sharp making exact determination of the retention time difficult. For this reason, its data point was omitted in the analysis of constant

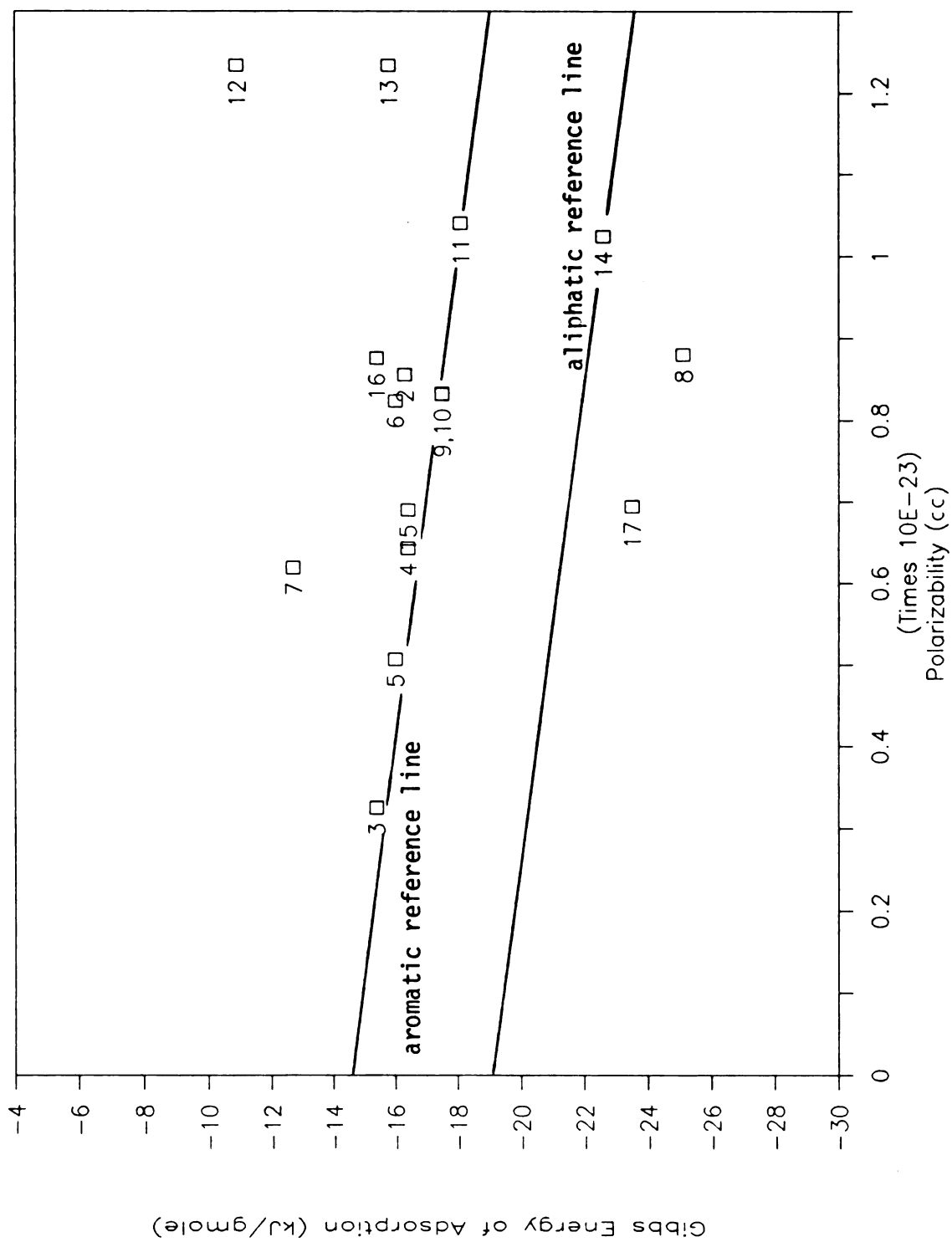


Figure 4. ΔG_{ads} vs. α_1 (8.4% coverage, 130°C)

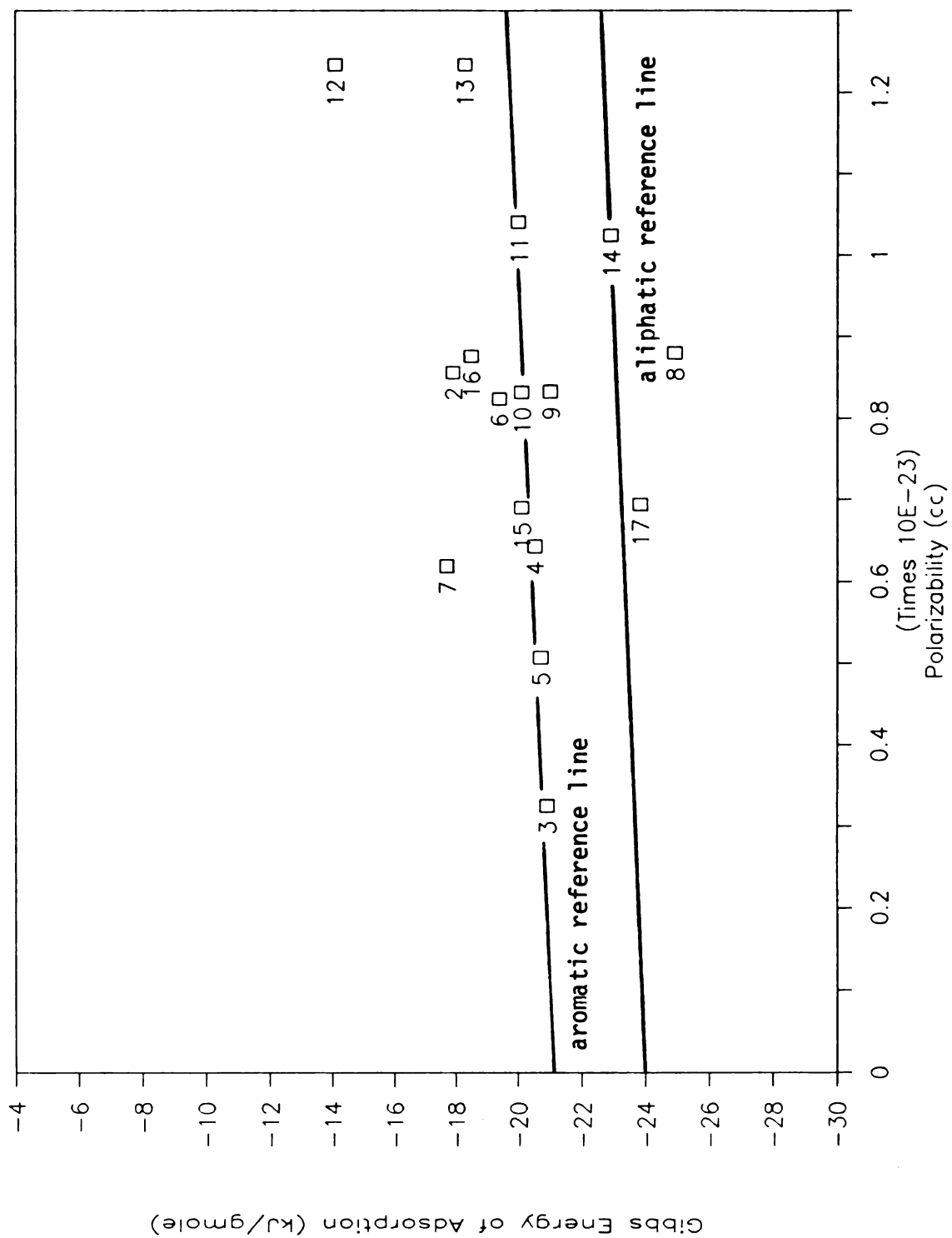


Figure 5. ΔG_{ads} vs. α_1 (8.4% coverage, 160°C)

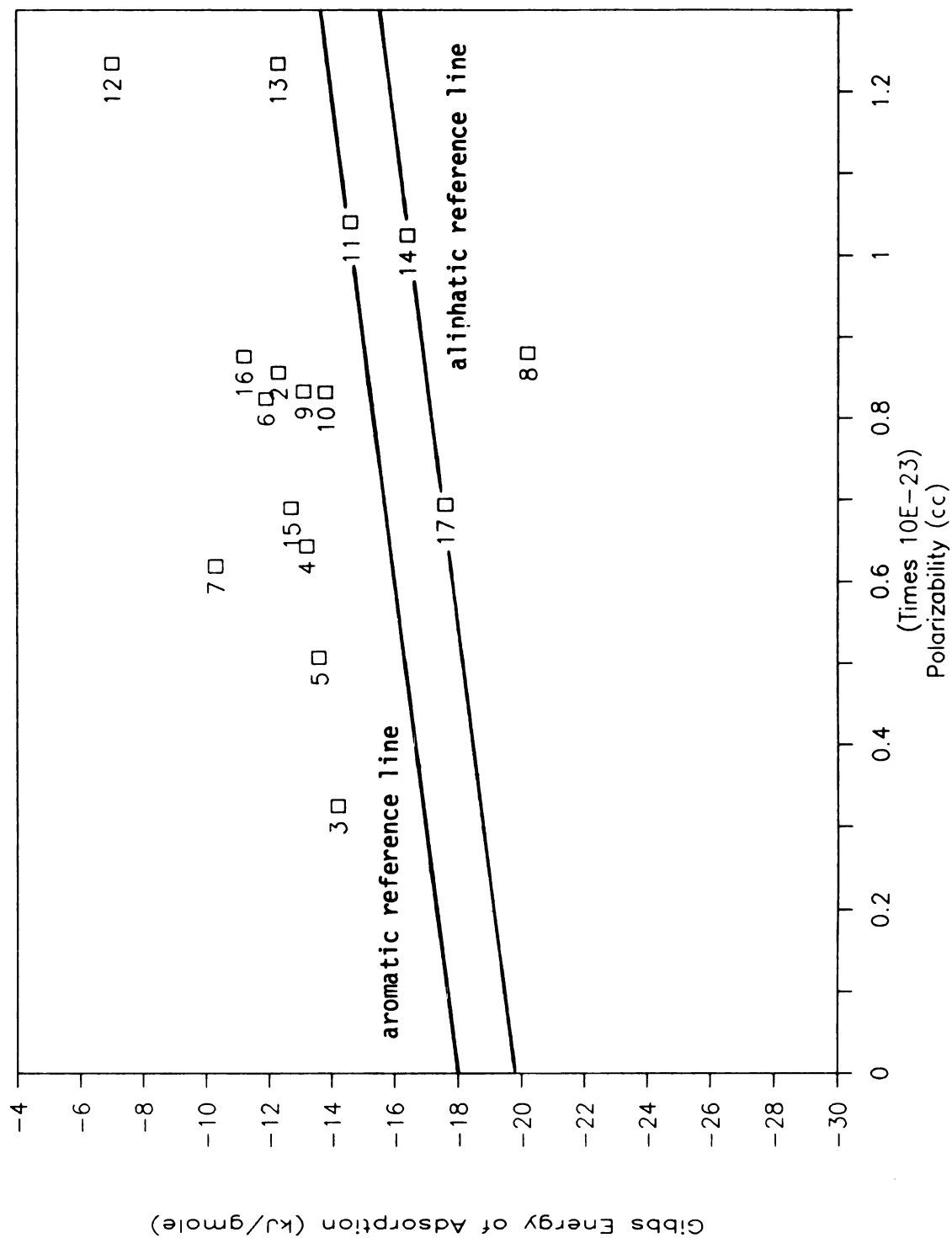


Figure 6. ΔG_{ads} vs. α_1 (3.96% coverage, 130°C)

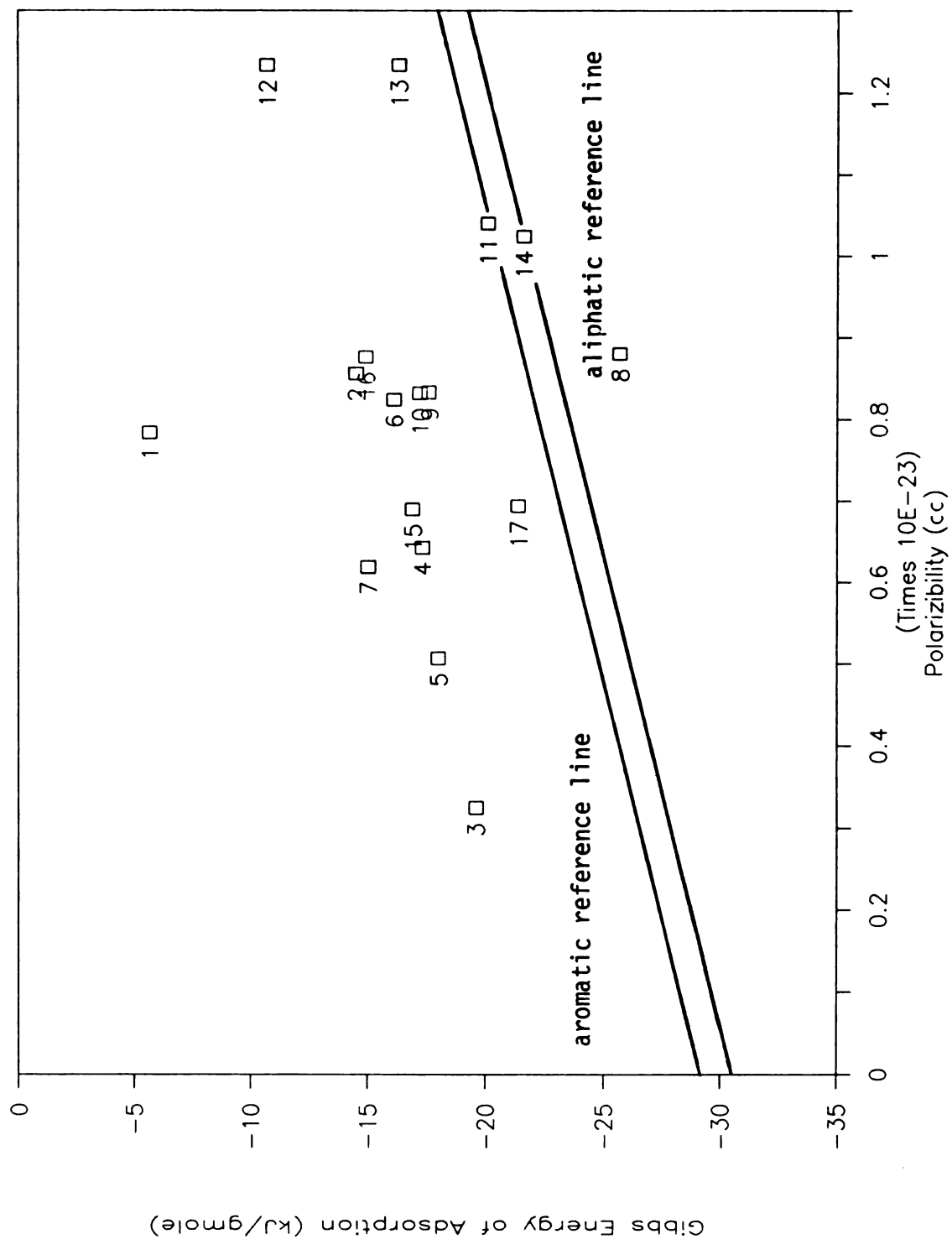


Figure 7. ΔG_{ads} vs. α_1 (3.96% coverage, 160°C)

b. A least-squares method using a Y-intercept forced to be equal to zero, was used to determine the slope of the line, b. The equations describing this set of reference lines, and the respective standard deviations, s, are:

$$\Delta G_{ad} (130^{\circ}\text{C}, 8.4\% \text{ cvg.}) = 6.29 \times 10^{29} \mu_1 \quad (54)$$

$$s = 1.4 \text{ kJ/gmole}$$

$$\Delta G_{ad} (160^{\circ}\text{C}, 8.4\% \text{ cvg.}) = 3.96 \times 10^{29} \mu_1 \quad (55)$$

$$s = 0.88 \text{ kJ/gmole}$$

$$\Delta G_{ad} (130^{\circ}\text{C}, 3.96\% \text{ cvg.}) = 5.48 \times 10^{29} \mu_1 \quad (56)$$

$$s = 0.78 \text{ kJ/gmole}$$

$$\Delta G_{ad} (160^{\circ}\text{C}, 3.96\% \text{ cvg.}) = 7.97 \times 10^{29} \mu_1 \quad (57)$$

$$s = 0.65 \text{ kJ/gmole}$$

Values of ΔG_{ads} calculated using the model and appropriate values for constants a, b, and c are identified as ΔG_{ads}^* in Tables 13 through 16. Finally, the difference between ΔG_{ads} obtained from experimental data and ΔG_{ads}^* results in the specific interaction parameter, Λ . The values of Λ are also included in Tables 13 through 16.

4.3.4. Dependence of Solubility on Thermodynamic Parameters

Tables 17 through 20 summarize the results of this work for each temperature and coverage ratio. The tables contain values for the

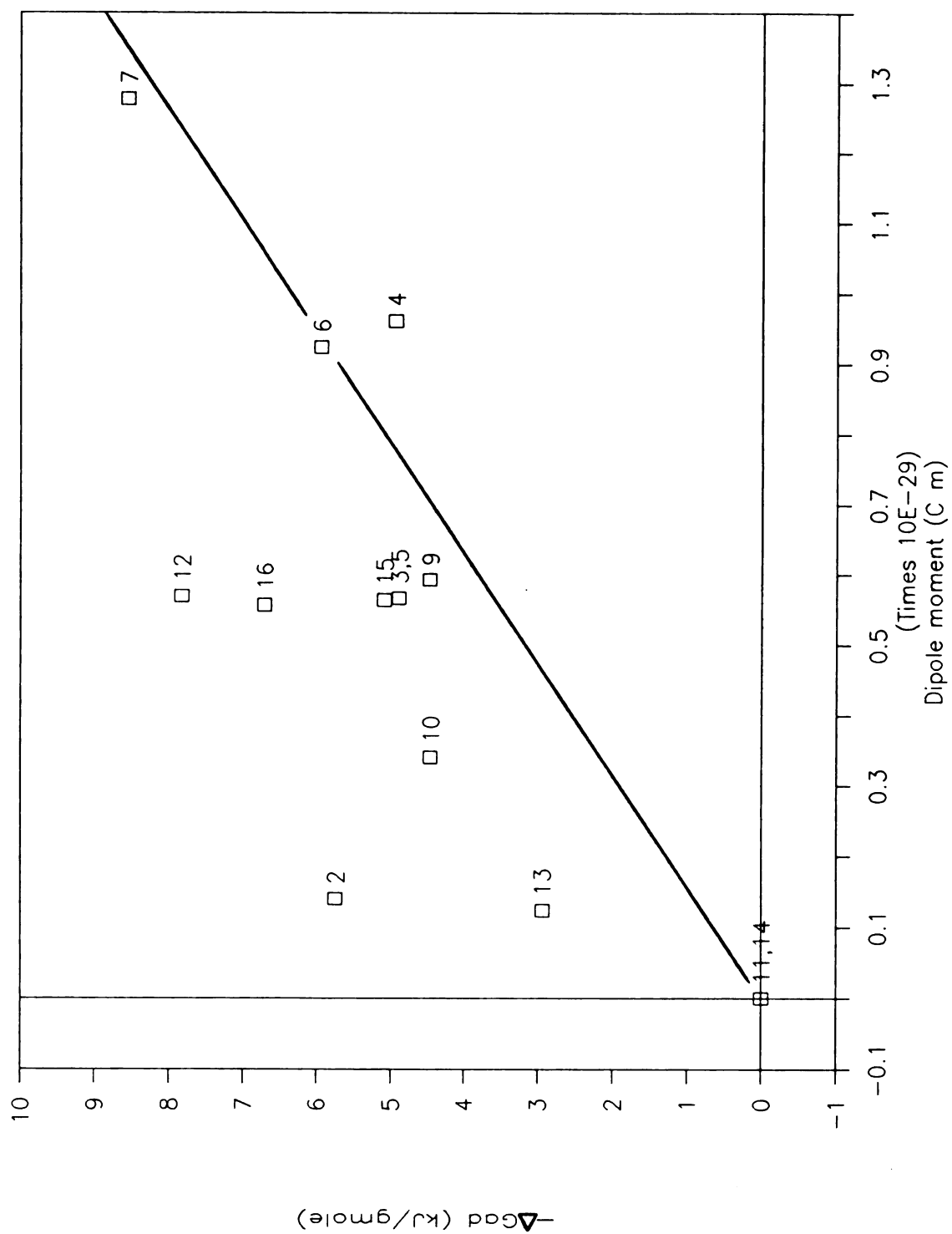


Figure 8. ΔG_{ad} vs. μ_1 (8.4% coverage, 130°C)

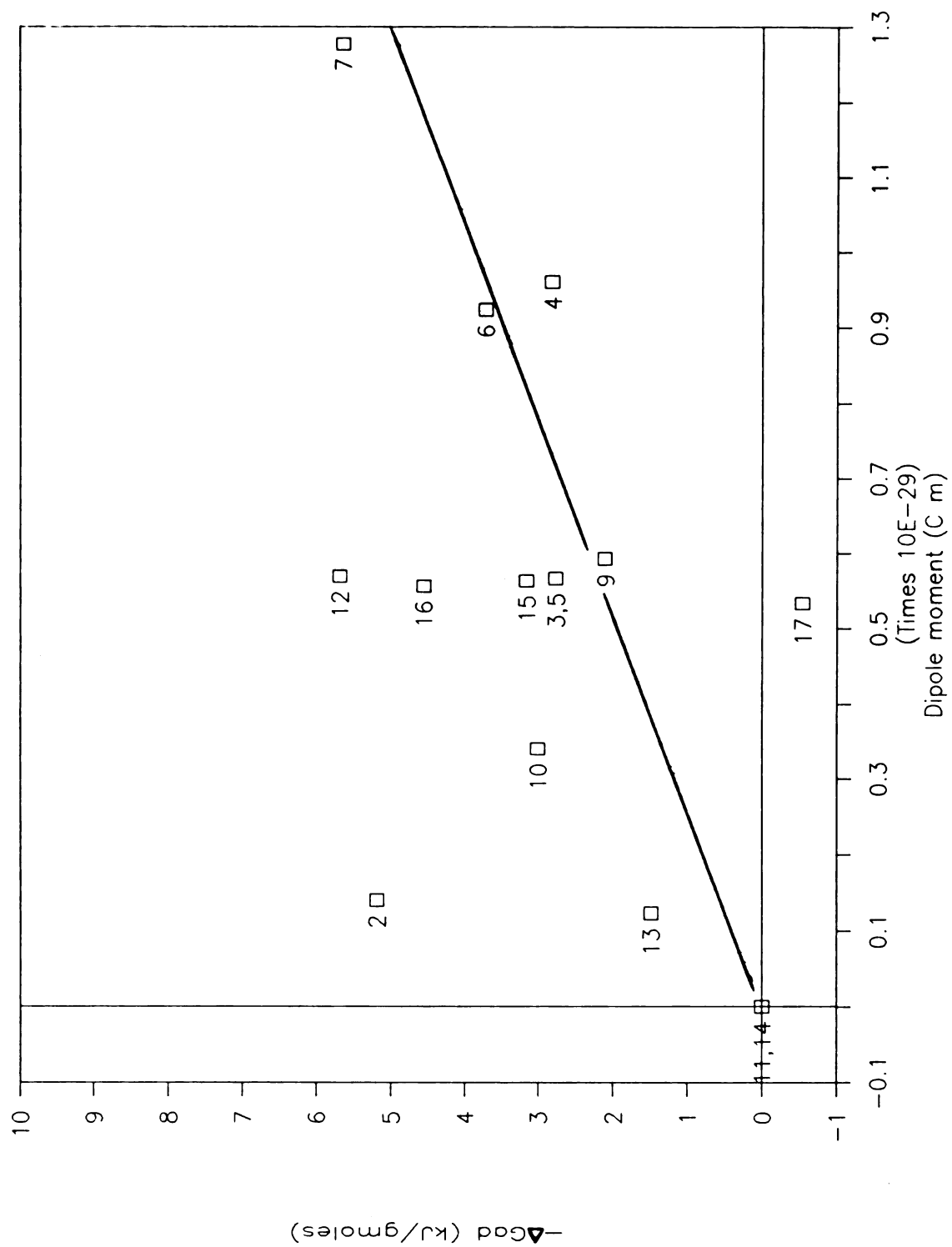


Figure 9. ΔG_{ad} vs. μ_1 (8.4% coverage, 160°C)

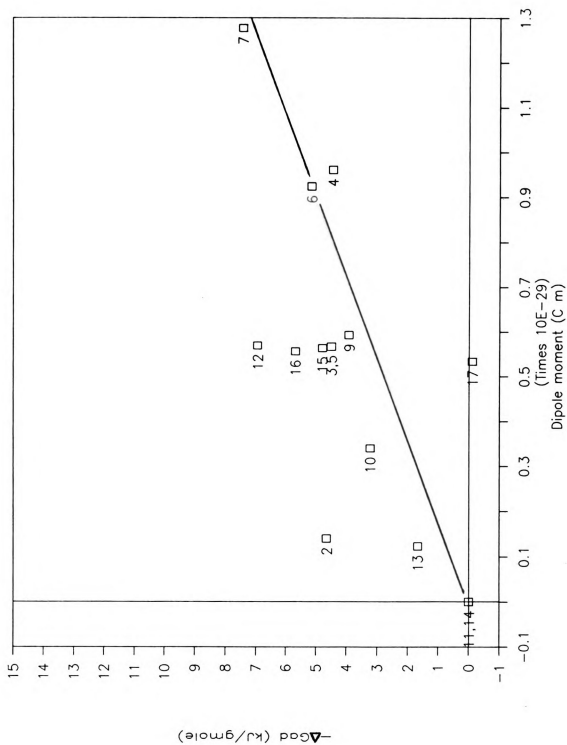


Figure 10. ΔG_{ad} vs. μ_1 (3.96% coverage, 130°C)

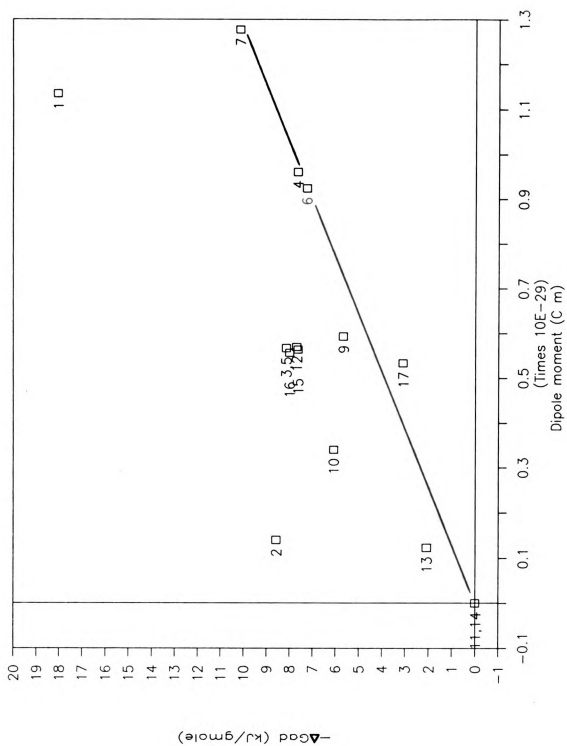


Figure 11. ΔG_{ad} vs. μ_1 (3.96% coverage, 160°C)

solubility parameter, the Flory-Huggins interaction parameter, χ , and the specific interaction parameter, Λ . As previously stated, conclusions regarding solubility must be made by carefully interpreting these three thermodynamic quantities. Although quantitative conclusions are difficult to arrive at it must be remembered that the motivation for using inverse GSC is to rapidly screen potential solvents for a given macromolecule.

Classically, the Flory-Huggins interaction parameter serves as an indication of whether a solvent can dissolve a polymer or not. By definition χ represents the energetic interactions in a polymer solution. However, in this work the polymer of interest was studied at temperatures less than the glass transition temperature and χ is interpreted to represent the molecular interactions between the solid support and a gaseous solvent. Calculation of χ from equation 24 utilizes liquid molar volumes for a gas-solid system and may result in some ambiguity in the values of the Flory-Huggins interaction parameters. For this reason, the values of χ calculated should be used to compare results for different solvents rather than interpreting single values of χ . All of the χ values calculated are positive; low positive values indicate that interactions are favorable and relatively high values of χ imply that interaction between the solvent and polymer is less likely.

Relatively high values of the specific interaction parameter, Λ , also indicate that a particular compound may serve as a solvent for the polymer. Neither the Flory-Huggins interaction parameter or the specific interaction parameter can conclusively determine if a solvent will, in

Table 17. Summary of Results for 8.4% Coverage at 130°C

<u>Solvent</u>	δ_1 <u>(cal/cc)^{1/2}</u>	<u>χ</u>	<u>Δ</u> <u>(kJ/gmole)</u>
2 Dioxane	10.00	3.33	4.87
3 Methanol	14.51	1.45	1.33
4 Acetone	10.00	1.73	-1.09
5 Ethanol	12.90	1.99	1.33
6 Methyl ethyl ketone	9.30	2.29	0.129
7 Acrylonitrile	11.00	1.36	0.533
8 Diethyl ether	7.40	3.69	-5.38
9 Ethyl acetate	9.10	2.82	0.740
10 Chloroform	9.30	2.94	2.33
11 Benzene	9.15	3.16	0
12 Chlorobenzene	9.50	2.69	4.25
13 Toluene	8.90	3.30	2.17
14 Carbon tetrachloride	8.60	5.05	0
15 n-Propanol	12.05	2.80	1.55
16 n-Butanol	11.40	3.22	3.20
17 i-Propanol	11.60	4.30	-5.34

Table 18. Summary of Results for 8.4% Coverage at 160°C

<u>Solvent</u>	<u>δ_1 (cal/cc)^{1/2}</u>	<u>χ</u>	<u>Δ (kJ/gmole)</u>
2 Dioxane	10.00	2.68	4.63
3 Methanol	14.51	1.81	0.526
4 Acetone	10.00	1.80	-0.98
5 Ethanol	12.90	2.09	0.526
6 Methyl ethyl ketone	9.30	2.16	0.066
7 Acrylonitrile	11.00	1.73	0.595
8 Diethyl ether	7.40	2.42	-3.36
9 Ethyl acetate	9.10	2.65	-0.24
10 Chloroform	9.30	2.61	1.67
11 Benzene	9.15	2.62	0
12 Chlorobenzene	9.50	2.55	3.43
13 Toluene	8.90	2.76	1.00
14 Carbon tetrachloride	8.60	3.97	0
15 n-Propanol	12.05	2.57	0.937
16 n-Butanol	11.40	2.80	2.36
17 i-Propanol	11.60	3.01	-2.65

Table 19. Summary of Results for 3.96% Coverage at 130°C

<u>Solvent</u>	<u>δ_1 (cal/cc)^{1/2}</u>	<u>χ</u>	<u>Δ (kJ/gmole)</u>
2 Dioxane	10.00	2.15	3.89
3 Methanol	14.51	1.08	1.40
4 Acetone	10.00	.800	-0.80
5 Ethanol	12.90	1.28	1.40
6 Methyl ethyl ketone	9.30	1.10	0.098
7 Acrylonitrile	11.00	.655	0.441
8 Diethyl ether	7.40	2.23	-5.42
9 Ethyl acetate	9.10	1.49	0.681
10 Chloroform	9.30	1.85	1.37
11 Benzene	9.15	2.13	0
12 Chlorobenzene	9.50	1.52	3.83
13 Toluene	8.90	2.26	0.986
14 Carbon tetrachloride	8.60	3.18	0
15 n-Propanol	12.05	1.70	1.71
16 n-Butanol	11.40	1.95	2.64
17 i-Propanol	11.60	2.56	-3.03

Table 20. Summary of Results for 3.96% Coverage at 160°C

<u>Solvent</u>	<u>δ_1 (cal/cc)^{1/2}</u>	<u>χ</u>	<u>Δ (kJ/gmole)</u>
1 Dimethylformamide	11.80	.513	9.01
2 Dioxane	10.00	1.74	7.46
3 Methanol	14.51	1.45	3.62
4 Acetone	10.00	.925	-0.01
5 Ethanol	12.90	1.35	3.62
6 Methyl ethyl ketone	9.30	1.24	-0.01
7 Acrylonitrile	11.00	.994	-0.02
8 Diethyl ether	7.40	2.64	-5.89
9 Ethyl acetate	9.10	1.70	0.951
10 Chloroform	9.30	1.81	3.34
11 Benzene	9.15	2.63	0
12 Chlorobenzene	9.50	1.59	3.15
13 Toluene	8.90	2.19	1.11
14 Carbon tetrachloride	8.60	3.60	0
15 n-Propanol	12.05	1.69	3.14
16 n-Butanol	11.40	1.79	3.56
17 i-Propanol	11.60	2.35	-1.15

fact, dissolve a polymer. The two thermodynamic quantities must be analyzed in conjunction with the solubility parameter in order that appropriate conclusions be drawn.

From bench scale solubility studies the best solvent tested was found to be dimethylformamide. Kraft lignin is soluble in dimethylformamide at concentrations greater than 10% by weight. The χ value for DMF at 160°C for 3.96% coverage ratio is very low relative to the other compounds studied and, at the same time, the specific interaction parameter is relatively high; both strong indications that interaction is occurring. The solubility parameter for DMF is $11.80 \text{ (cal/cc)}^{1/2}$ which is approximately the value determined by Schuerch to correspond for kraft lignin [Schuerch, 1952].

It is helpful to display the data in graphical form by plotting Δ versus χ at each temperature and column loading. The four graphs depicting this can be found in Figures 12 through 15. It can be seen in each of these figures that the points for compounds which form solutions of greater than 1% by weight with lignin are very near to each other. In addition, most of these points are located in the left upper quadrant of the graph where Δ is maximized and χ is minimized. Data points for dioxane and chlorobenzene represent the only exceptions.

Dioxane has a very high value of the specific interaction parameter when compared to the other data but its Flory-Huggins interaction parameter is similar to that of many non-solvents. In this case the very high value of Δ and a solubility parameter for dioxane equal to $10 \text{ (cal/cc)}^{1/2}$ is

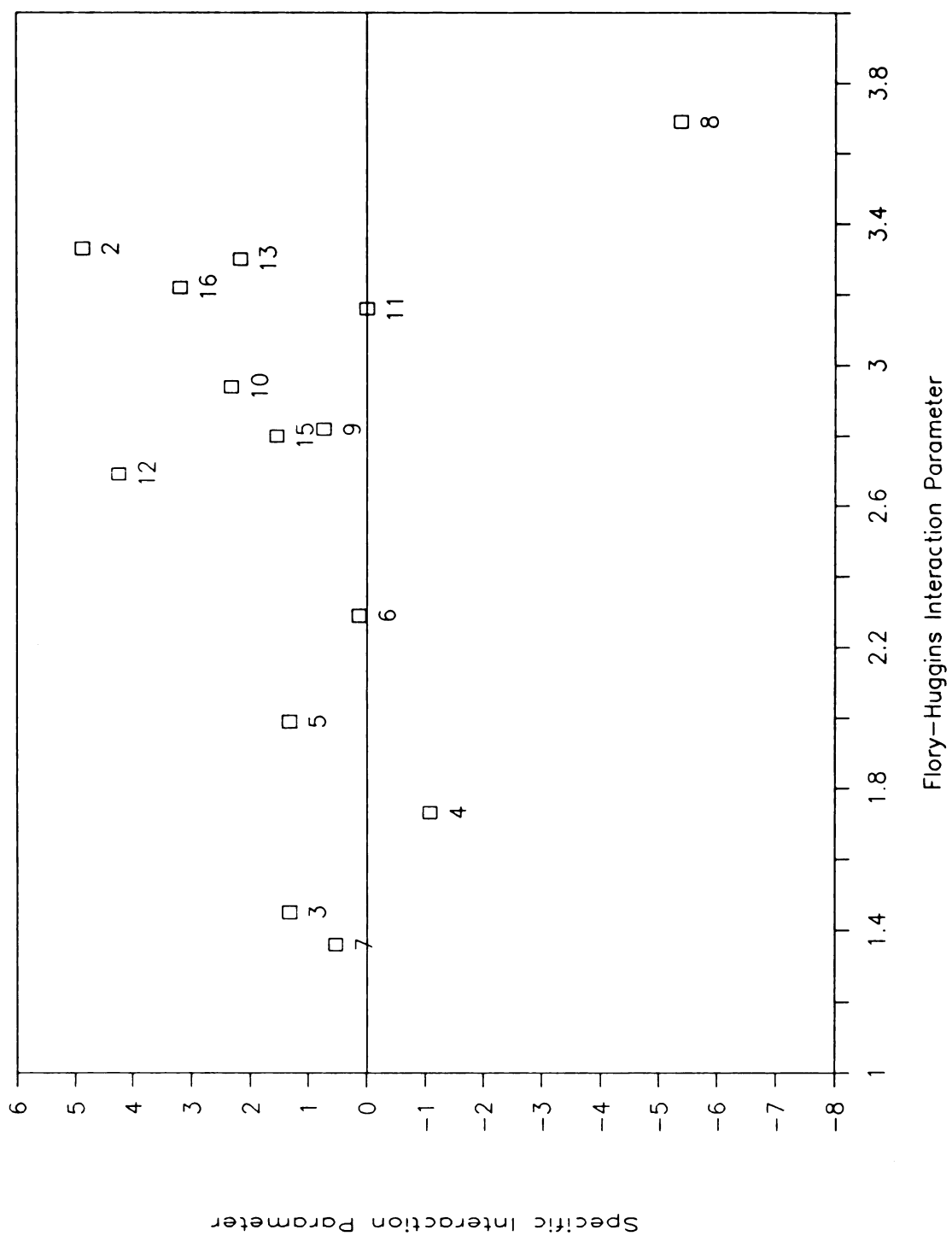


Figure 12. χ versus χ for 8.4% Coverage and 130°C

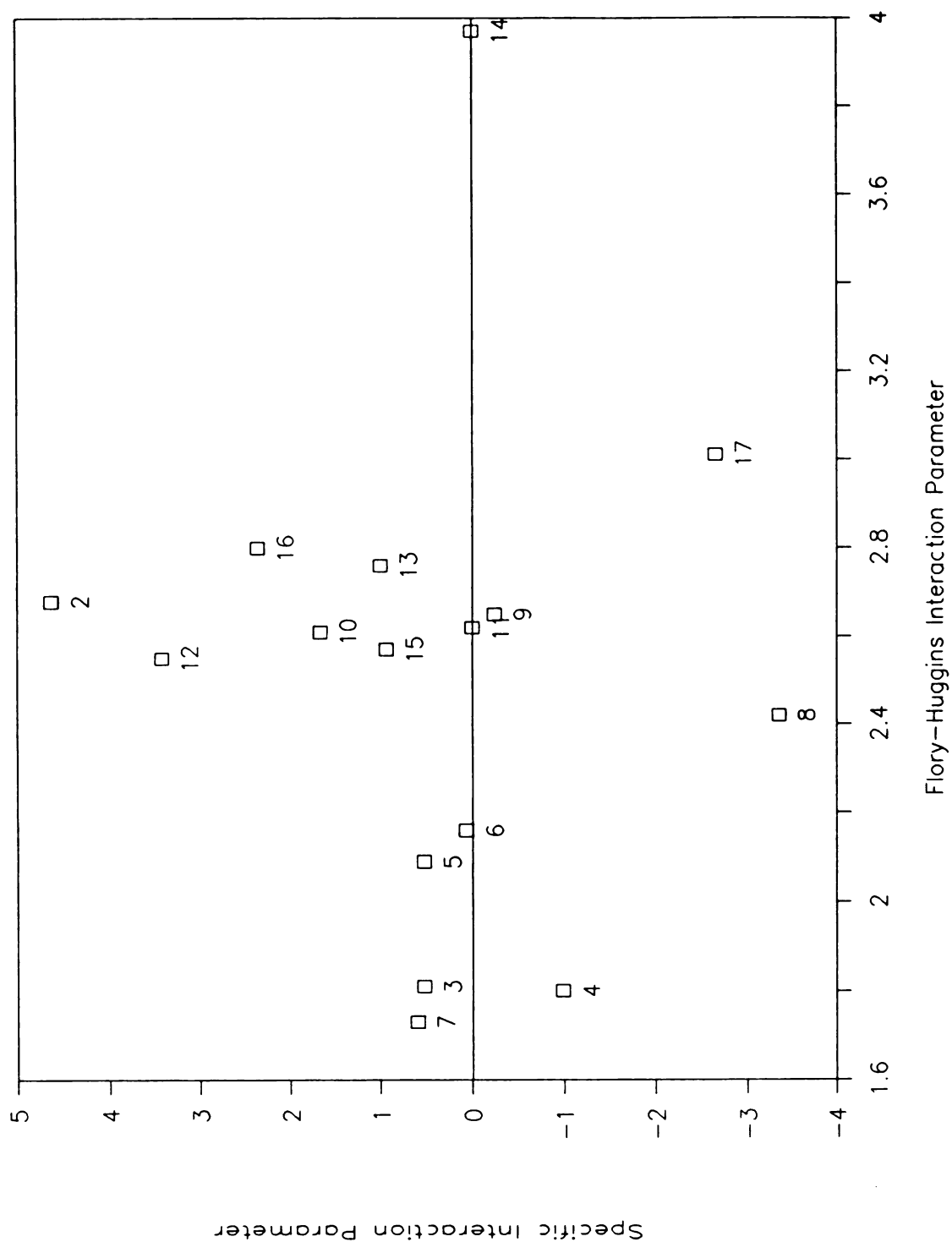


Figure 13. Λ versus χ for 8.4% Coverage and 160°C

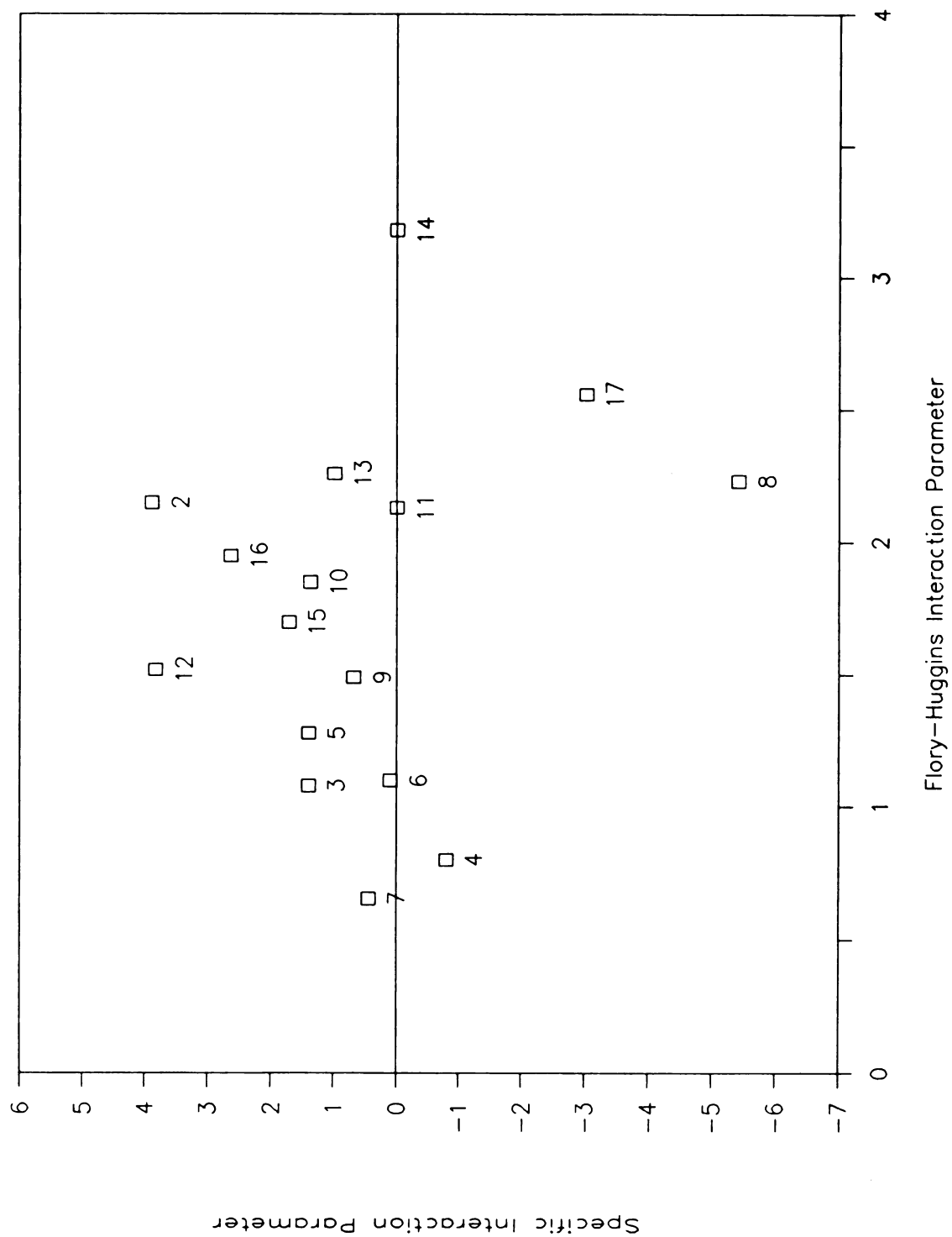


Figure 14. Λ versus χ for 3.96% Coverage and 130°C

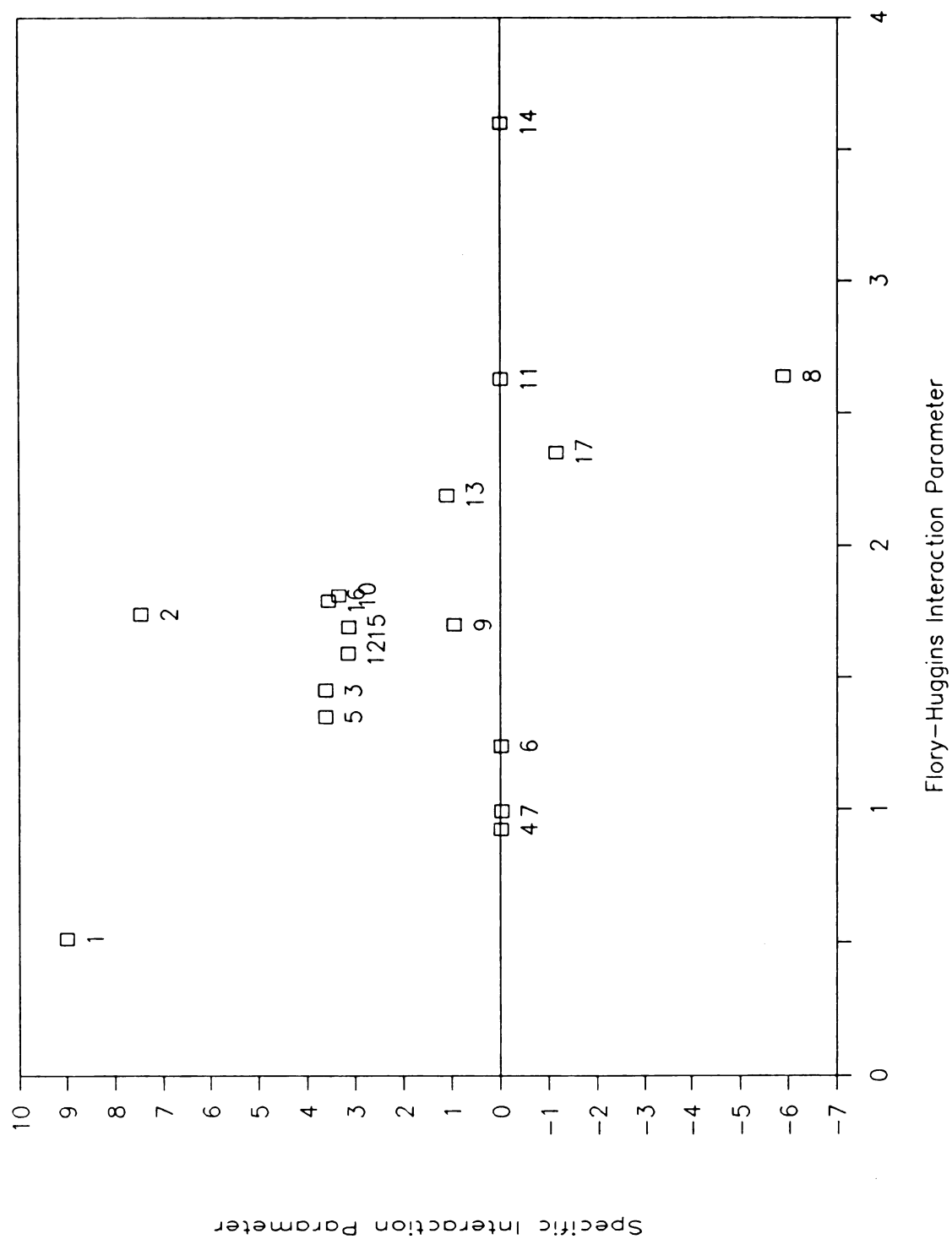


Figure 15. Δ versus χ for 3.96% Coverage and 160°C

sufficient to indicate that dioxane is a potential solvent for kraft lignin. This conclusion is further emphasized by the data depicted graphically in Figure 15. Data for dimethylformamide as well as dioxane is available for the column packed at 3.96% coverage and operating at a column temperature of 160°C. It is obvious that both these points lie far above (ie. much higher values of Λ) all the other data points.

The data collected for chlorobenzene is subject to suspect. Firstly, the boiling point of chlorobenzene is just above 130°C. Any condensation of chlorobenzene in the column would explain why the chromatograms did not exhibit sharp peaks. Non-symmetrical, drawn-out peaks result in retention times which are difficult to reproduce.

The experiments at 160°C for chlorobenzene yielded chromatograms with well-defined, sharp peaks. This leads to reproducible retention times and therefore, better estimates of the Flory-Huggins interaction parameter and the specific interaction parameter. In Figures 13 and 15 it is seen that the chlorobenzene data point is near the cluster of data representing the non-solvents. However, based on this data further investigation of chlorobenzene as a potential solvent for kraft lignin is warranted.

4.3.5. Dependence of χ and Λ on Operating Conditions

Collecting data at two column temperatures and two column loadings allows for comparisons to be made based on operating conditions. Figures 12

through 15 demonstrate that the trend of the data is consistent as changes are made in each of the above parameters.

Values of the specific interaction parameter generally increase as temperature increases or column loadings decrease. Although there are some obvious exceptions it is no surprise that the dependence of Λ on these parameters is not well-defined. The exact nature of the specific interactions and their subsequent dependence on temperature are a continuing subject of debate therefore, generalities regarding these dependencies are difficult to arrive at.

Initially it appears that the Flory-Huggins interaction parameter depends on the column loading. Since χ represents molecular interactions in a polymer solution this dependence is unrealistic. Upon further examination it can be seen that the ratio of $\chi(3.96\%)/\chi(8.4\%)$ is the same for all the solvents at both 130°C and 160°C. As discussed previously, the use of liquid molar volumes in equation 24 to calculate χ values for a gas-solid system can lead to some discrepancies. Additionally, the value of the specific volume of the polymer, v_2 , was experimentally determined at room temperature instead of at each of the column operating temperatures. For these reasons it should again be emphasized that the comparisons of χ values be limited to a given set of column operating conditions.

As indicated by the data in Tables 17 through 20 the Flory-Huggins interaction parameter does not exhibit a strong temperature dependence.

Many of the differences in the values of χ as the temperature is increased from 130°C to 160°C are slight.

V. Summary and Conclusions

The method of inverse gas-solid chromatography was used to assess the solubility characteristics of 17 solvents with kraft lignin. Flory-Huggins interaction parameters and specific interaction parameters were determined at two column operating temperatures and two column loadings.

The high solubility of kraft lignin in dimethylformamide is predicted by this method based on the values of χ , Δ , and the solubility parameter of DMF. The trend of the data acquired from inverse GSC experiments is supported by bench scale solubility studies performed at room temperature.

Calculation of the Flory-Huggins interaction parameter for a gas-solid system does provide useful information regarding energetic interactions between the polymer and the solvent. Although specific values for the Flory-Huggins interaction parameter can not be obtained from GSC, the calculated values can be used to interpret data within an experimental set of conditions.

The method of inverse GSC was shown to provide a simple, rapid, and accurate screening tool for potential solvents for a complex, non-crystalline, network polymer such as lignin.

Since lignin is an abundant, renewable resource it is seeing concentrated efforts to develop usable materials such as adhesives, fillers, and chemical feedstocks via chemical modification. The method of inverse GSC will be extremely useful for determining solvents for the wide variety of lignins resulting from these modification reactions.

LIST OF REFERENCES

LIST OF REFERENCES

- Braddon, D. V. and S. I. Falkehag. "Torsional Braid Analysis of Lignin Derived Rubber Stabilizers." *Journal of Polymer Science: Symposium*, no. 40, 101, (1973).
- Brockmeier, N. F., R. W. McCoy, and J. A. Meyer. "Gas Chromatographic Determination of Thermodynamic Properties of Polymer Solutions. I. Amorphous Polymer Systems." *Macromolecules*, 5(4),464, (1972).
- Chang, Y. H. and D. C. Bonner. "Sorption of Solutes by Poly(ethylene oxide) I. Infinite-Dilution Studies." *Journal of Applied Polymer Science*, 19, 2439, (1975).
- Chow, S.. "Adhesive Developments in Forest Products." *Wood Science and Technology*, 17, 1, (1983).
- Clarke, J. Peter. "How to Design Chemical Plants on the Back of an Envelope." *Chemtech*, April, 1976, pg. 235.
- Conder, John R.. "Teflon, A Noninert Chromatographic Support." *Analytical Chemistry*, 43, 367, (1971).
- Connors, W. J., L. N. Johanson, K. V. Sarkanen, and P. Winslow. "Thermal Degradation of Kraft Lignin in Tetralin." *Holzforschung*, 34, 29, (1980).
- Dangayach, K. C. B., K. A. Karim and D. C. Bonner. "Interactions of Organic Solvents with Aromatic Heterocyclic Polymers I. m-Phenylene Polybenzimidazole." *Journal of Applied Polymer Science*, 26, 559, (1981).
- Defaye, Jacques, Andree Gadelle, John Papadopoulos and Christian Pedersen. "Hydrogen Fluoride Saccharification of Cellulose and Lignocellulosic Materials." *Journal of Applied Polymer Science: Applied Polymer Symposium*, no. 37, 653, (1983).
- Del Gatto, Joseph V., Ed.. "Lignin Shows Commercial Promise as Reinforcer." *Rubber World*, February, 1972, pg. 49.
- Dincer, S. and D. C. Bonner. "Solubility Criteria for a Thermally Stable Polymer Determined by Gas-Solid Chromatography." *Journal of Applied Polymer Science*, 22, 3235, (1978).

- Dincer S. and D. C. Bonner. "Thermodynamic Analysis of an Ethylene and Vinyl Acetate Copolymer with Various Solvents by Gas Chromatography." *Macromolecules*, 11(1), 107, (1978).
- Dolenko, A. J. and M. R. Clarke. "Resin Binders From Kraft Lignin." *Forest Products Journal*, 28(8), 41, (1978).
- Drew, Stephen W., Kiran L. Kadam, Sharon P. Shoemaker, W. G. Glasser, and P. Hall. "Chemical Feedstocks and Fuels from Lignin," *Biochemical Engineering: Renewable Sources*, AIChE Symposium Series, no. 181, 21, (1978).
- Dwyer, John and Khalid A. Karim. "New Approach to the Study of Solute-Solvent Interaction in a Gas Liquid Chromatography Column." *Industrial and Engineering Chemistry, Fundamentals*, 14, 196 (1975).
- Elder, T. J. and E. J. Soltes. "Adhesive Potentials of Some Phenolic Constituents of Pine Pyrolysis." Paper presented at the ACS National Meeting, Carbohydrate Chemistry Division, Washington, D.C., September 10-14, 1979.
- Era, Vanino A., and Jahka Hannula. "Polyesters From Vanillin. Synthesis and Characterization." *Paperi ja Puu*, 56(5), 489, (1974).
- Falkehag, S. I., D. V. Braddon and W. K. Dougherty. *Lignin Polymer Applications*. Westvaco Corporation, Charleston Research Center, 1976.
- Farmer, Robert H.. "Pulp and Paper Manufacture," chapter in *Chemistry in the Utilization of Wood*, New York: Wiley, pg. 143.
- Flory, P. J.. Principles of Polymer Chemistry. New York: Cornell Press, 1953.
- Forsman, W. R.. "Heating of Alkaline Birch Black Liquor." *Suomen Kemistiseuran Tiedonantoja*, 81, 47, (1972).
- Forss, Kaj G. and Agneta Fuhrmann. "Finnish Plywood, Particleboard, and Fiberboard Made with a Lignin-Base Adhesive." *Forest Products Journal*, 29(7), 39, (1979).
- Galin M. and M. C. Rupprecht. "Study by Gas-Liquid Chromatography of the Interactions Between Linear or Branched Polystyrenes and Solvents in the Temperature Range 60° to 200°C." *Polymer*, 19, 506, (1978).
- Glasser, Wolfgang G., Charlotte A. Barnett, Timothy G. Rials, and Basudew P. Saraf. "Engineering Plastics from Lignin. II. Characterization of Hydroxyalkyl Lignin Derivatives." *Journal of Applied Polymer Science*, 29, 1815, (1984).
- Glasser, Wolfgang G.. "Potential Role of Lignin in Tomorrow's Wood Utilization Technologies." *Forest Products Journal*, 31(3), 24, (1981).

- Go, T. A.. "Development of Lignin-Based Adhesives." Presentation at Symposium on Lignin Based Adhesives, 1980.
- Goheen and Martin, U. S. Patent 3375283.
- Goheen, D. W.. "Hydrogenation of Lignin by the NOGUCHI Process." Advances in Chemistry, series 59, 205, (1966).
- Gordy, Walter and Speacer C. Stanford. "Spectroscopic Evidence for Hydrogen Bonds: Comparison of Proton-Attracting Properties of Liquids III.." Journal of Chemistry and Physics, 9, 204, (1941).
- Gray, D. G. and J. E. Guillet. "A Gas Chromatographic Method for the Study of Sorption on Polymers." Macromolecules, 3(3), 316, (1972).
- Guillet, James E.. "Molecular Probes in the Study of Polymer Structure." Journal of Macromolecular Science--Chemistry, A4(7), 1669, (1970).
- Guillet, James E.. "Study of Polymer Structure and Interactions by Inverse Gas Chromatography," in Progress in Gas Chromatography. Ed. H. Purnell. New York: Wiley, 1973.
- Hsu, Oscar H.-H. and Wolfgang G. Glasser. "Polyurethane Adhesives and Coatings from Modified Lignin." Wood Science, 9(2), 97, (1976).
- Hsu, Oscar H.-H. and Wolfgang G. Glasser. "Polyurethane Foams from Carboxylated Lignins." Applied Polymer Symposium, no. 28, 297, (1975).
- Huibers, Derek. Hydrocarbon Research, at panel discussion, NSF-Lignin Symposium, Battelle Columbus Laboratory, Columbus, Ohio, October 10-11, 1979.
- Janshekar, H. and A. Fiechter. "Lignin: Biosynthesis, Application, and Biodegradation." Advances in Biochemical Engineering: Biotechnology, 27, 119, (1983).
- Karim, Khalid A. and David C. Bonner. "Thermodynamic Interpretation of Solute-Polymer Interactions at Infinite Dilution." Journal of Applied Polymer Science, 22, 1277, (1978).
- Kilpelainen, Harri, Kaj Forss, and Agneta Fuhrmann. "Lignin-Based Adhesives for the Board Industry." Proceedings of the IUFRO Conference on Wood Gluing, 1975, Helsinki, Finland, published 1976.
- Lindberg, J. Johan, Vaino A. Era, Tuure P. Jauhiainen. "Lignin as a Raw Material for Synthetic Polymers." Applied Polymer Symposium, no. 28, 269, (1975).
- Maryott, A. A., and F. Buckley. National Bureau of Standards Circular, U.S. Government Printing Office, Washington, D.C., 537, (1953).
- Mischustin, I. U.. "Light Fillers for Rubber". Caoutchouc and Rubber, 9, 39 (1940).

- Newman, R. D. and J. M. Prausnitz. "Polymer Solvent Interactions from Gas-Liquid Chromatography." *Journal of Paint Technology*, 45(585), 33, (1973).
- Newman, R. D. and J. M. Prausnitz. "Polymer-Solvent Interactions from Gas-Liquid Partition Chromatography." *The Journal of Physical Chemistry*, 76(10), 1492, (1972).
- Newman, R. D. and J. M. Prausnitz. "Thermodynamics of Concentrated Polymer Solutions Containing Polyethylene, Polyisobutylene, and Copolymers of Ethylene with Vinyl Acetate and Propylene." *AIChE Journal*, 19(4), 704, (1973).
- O'Connell, J. P., and J. M. Prausnitz. "Empirical Correlation of Second Virial Coefficients for Vapor-Liquid Equilibrium Calculations." *Industrial and Engineering Chemistry, Process Design and Development*, 6(2), 245, (1967).
- Patterson D.. "Free Volume and Polymer Solubility. A Qualitative View." *Macromolecules*, 22(6), 672, (1969).
- Patterson, D., Y. B. Tewari, H. P. Schreiber, and J. E. Guillet. "Application of Gas-Liquid Chromatography to the Thermodynamics of Polymer Solutions." *Macromolecules*, 4(3), 356, (1971).
- Penttinen, K.. "Reactivities of Nitrophenyl Nitrobenzoates and Aminophenyl Aminobenzoates in Relation to Polypyromellitimide Formation". Dissertation, University of Helsinki, 1970.
- Pitzer, K. S., and R. F. Curl, Jr.. "Empirical Equation for the Second Virial Coefficient." *Journal of the American Chemical Society*, 79, 2369, (1957).
- Prigogine, I.. The Molecular Theory of Solutions. Amsterdam: North-Holland Press, 1957.
- Raff, R. A. V., G. H. Tomlinson II, T. L. Davies and W. H. Watson. "Oxidized Lignin as a Reinforcing Agent for Rubber." *Rubber Age*, November, 1948, pg. 197.
- Reid, Robert C., John M. Prausnitz, and Thomas K. Sherwood. The Properties of Gases and Liquids. 3rd edition. New York: McGraw-Hill, 1977.
- Roberts, John. Westvaco Chemicals Corporation, Kraft Division, P.O. Box 5207, North Charleston, SC 29406. Phone Consultation, 1987.
- Sarkanen, K. V. and C. H. Ludwig. Lignins: Occurrence, Formation, Structure, and Reactions. New York: Wiley, 1971.
- Schreiber, H. P., T. B. Tewari, and D. Patterson. "Thermodynamic Interactions in Polymer Systems by Gas-Liquid Chromatography. III. Polyethylene Hydrocarbons." *Journal of Polymer Science: Polymer Physics Edition*, 11, 15, (1973).

- Schuerch, Conrad. "The Solvent Properties of Liquids and Their Relation to the Solubility, Swelling, Isolation and Fractionation of Lignin." *Journal of the American Chemical Society*, 74, 5061, (1952).
- Schweers, W.. "On the Hydrogenolysis of Lignin. II. Hydration of Different Lignins with Complex Compounds of the Transition Elements, Iron, Cobalt, and Nickel as Catalysts." *Holzforschung*, 23(1), 5, (1969).
- Selke, Susan M., Martin C. Hawley, Haim Hardt, Derek T. A. Lamport, Gary Smith, and James Smith. "Chemicals from Wood via HF." *Industrial and Engineering Chemistry, Product Research and Development*, 21(1), 11, (1982).
- Shen, K. C. and D. P. C. Fung. "Aspen Particleboards Bonded With Spent Sulfite Liquor Powder Treated With Sulfuric Acid." *Forest Products Journal*, 29(3), 34, (1979).
- Smidsrod, Olav, and J. E. Guillet. "Study of Polymer-Solute Interactions by Gas Chromatography." *Macromolecules*, 2, 272, (1969).
- Smith, James J., Derek T. A. Lamport, Martin C. Hawley, and Susan M. Selke. "Feasibility of Using Anhydrous Hydrogen Fluoride to 'Crack' Cellulose." *Journal of Applied Polymer Science: Applied Polymer Symposium*, no. 37, 641, (1983).
- Summers, W. R., Y. B. Tewari, and H. P. Schreiber. "Thermodynamic Interaction in Polydimethylsiloxane -Hydrocarbon Systems from Gas-Liquid Chromatography." *Macromolecules*, 5(1), 12, (1972).
- Timmermans, Jean. Physico-Chemical Constants of Binary Systems in Concentrated Solutions, Volumes I and II.. New York: Interscience Publishing, 1959.
- Tsonopoulos, Constantine. "An Empirical Correlation of Second Virial Coefficients." *AIChE Journal*, 20(2), 263, (1974).
- Yaws, Carl L.. Physical Properties. New York: McGraw-Hill, 1977.